Type of Article: Research Article

Title: Tracking late-Quaternary extinctions in interior Alaska using megaherbivore bone remains and dung fungal spores

Authors: Keziah J. Conroy[1,2], Ambroise G. Baker[1,3 *], Vivienne J. Jones[1*], Maarten van Hardenbroek[4,5], Emma J. Hopla[4], Robert Collier[4], Adrian M. Lister [6], Mary E. Edwards[4]

[1] ECRC, Department of Geography, University College London, Gower Street, London, WC1E 6BT

[2] Leverhulme Centre for Human Evolutionary Studies, Henry Wellcome Building, Fitzwilliam Street, Cambridge, CB2 1QH

[3] School of Health and Life Science, Teesside University, Middlesbrough, TS1 3BX

[4] Geography and Environment, University of Southampton, Southampton, SO17 1BJ

[5] Geography Politics and Sociology, Newcastle University, Newcastle upon Tyne, NE1 7RU

[6] Department of Earth Sciences, Natural History Museum, London, SW7 5BD

* Corresponding authors:

Dr Baker: a.baker@tees.ac.uk +44 (0)164273 8208

Prof Jones: vivienne.jones@ucl.ac.uk +44 (0)20 7679 0555

ABSTRACT

One major challenge in the study of late-Quaternary extinctions (LQE) is providing better estimates of past megafauna abundance. To show how megaherbivore population size varied before and after the last extinctions in interior Alaska, we use both a database of radiocarbon-dated bone remains (spanning 25-0 ka) and spores of the obligate dung fungus, *Sporormiella,* recovered from radiocarbon-dated lake-sediment cores (spanning 17-0 ka). Bone fossils show that the last stage of the LQE in the region occurred at about 13 ka ago, but the number of megaherbivore bones remains high into the Holocene. *Sporormiella* abundance also remains high into the Holocene and does not decrease with major vegetation changes recorded by arboreal pollen percentages. At two sites, the interpretation of *Sporormiella* was enhanced by additional dung fungal spore types (e.g. *Sordaria*). In contrast to many sites where the last stage of the LQE is marked by a sharp decline in *Sporormiella* abundance, in interior Alaska our results indicate the continuance of megaherbivore abundance, albeit with a major taxonomic turnover (including *Mammuthus* and *Equus* extinction) from predominantly grazing to browsing dietary guilds. This new and robust evidence implies that regional LQE events were not systematically associated with crashes of overall megaherbivore abundance.

Key words (10): Beringia, paleoecology, megafauna, herbivore, *Sporormiella*, *Sordaria*, coprophilous fungal spores, fossil, late glacial maximum, transition

INTRODUCTION

Late-Quaternary megafaunal extinctions (LQE) were a global, time-transgressive extinction wave that selectively affected megafauna (terrestrial vertebrates weighing >44kg) from 50 to 4 ka (Koch and Barnosky, 2006; Stuart, 2015). The causes and consequences of this are still extensively debated (Galetti et al., 2018; Gill, 2014; Hempson et al., 2015; Johnson, 2009; Malhi et al., 2016; Rabanus-Wallace et al., 2017; Sandom et al., 2014). In several regions of the world, such as Australia and North America, LQE appear approximately synchronous with human colonisation events; however, direct causality remains uncertain (e.g. Broughton and Weitzel, 2018; Johnson, 2009). Current research is actively exploring the consequences of LQE for ecosystem functioning and biodiversity. For example, the loss of key megaherbivores has been linked to changes in fire regimes (Gill, 2014), differences in nutrient cycling (Doughty et al., 2013) and dispersal limitation in certain plant species (Peres et al., 2016). Understanding both the causes and consequences of past megafaunal extinctions is important because extant megafauna is under threat of extinction today and is a strong focus of global nature conservation efforts.

One critical challenge in the study of LQE is a better understanding of past megafauna abundance (Bradshaw et al., 2003). Past distribution of megaherbivores is typically researched using radiocarbon-dated and identified bone remains recovered from, for example, archaeological sites, sedimentary deposits and caves. The main weaknesses of this evidence is that, to be compelling in terms of abundance, it needs to be based on extremely comprehensive collections as it focuses on presence of animal remains; absence of evidence cannot be taken as evidence of absence (Stuart, 2015). For example, low abundance may be undetected when using bone remains alone and can be mistaken for extinction events (Haile et al., 2009).

A useful methodology to address the presence/absence and abundance of megafauna uses the abundance of dung fungal spores along with fossil pollen recovered from sedimentary archives (Baker et al., 2016; Davis and Shafer, 2006; Gill et al., 2013). This method focuses on spores of ascomycete fungi whose life cycle is fully reliant on vertebrate herbivores and whose presence in sediments are consequently interpreted as compelling evidence for the presence of megaherbivores (Baker et al., 2013; Davis and Shafer, 2006; Johnson et al., 2015; van Geel et al., 2003). The spores produced during sexual reproduction are unintentionally ingested by megaherbivores while grazing. They subsequently germinate after digestion when deposited with dung. Depending on local conditions, such as moisture levels and temperature within the deposited dung, successful mycelium growth and fructification release explosively sticky spores onto surrounding vegetation, ready to be ingested. Some spores do not complete their biological cycle and are lost into the environment. A fraction of these lost spores will be integrated into sedimentary archives after transportation by turbulent air (Gill et al., 2013), water flow (Etienne et al., 2013) or slope run-offs (Baker et al., 2016). Despite the promise of this approach, there are some weaknesses, including the reliance on sampling sites such as lakes and bogs that may not be representative of the landscape. In addition, many studies using dung fungal spores rest on the identification of *Sporormiella* spores and do not include other types of dung fungal spores such as *Sordaria* and *Podospora* (Baker et al., 2013; Perrotti and van Asperen, 2019).

Radiocarbon-dated bone collections and dung fungal spores are complementary archives but are rarely applied together. However, there is the potential to develop such an approach where bone and spore results are directly compared, when the geographical relevance of both proxies is understood, for example, on islands (Graham et al., 2016) and in other isolated regions.

In North America, LQE were particularly severe, with 69% of megafauna species greater than 45 kg going extinct before the onset of the Holocene (Stuart, 2015). Most species survived until the Pleistocene-Holocene transition (14-10 ka) and dramatic megaherbivore losses, in terms of abundance, have been identified using *Sporormiella* at sites across North American (excluding east Beringia) at about 14 ka (Robinson et al., 2005, Davis and Shafer, 2006, Gill et al., 2009, Perrotti et al., 2018).

In northern Alaska and north-eastern Siberia, bone collections have been used to estimate temporal changes in faunal communities. Using a large database of radiocarbon-dated megaherbivore remains from the Alaska North Slope, Mann et al. (2013) suggest that between 45 and 10 ka there were 6 times more individuals and 30 times greater biomass of megaherbivores than at present. Dominant taxa were chiefly *Mammuthus* (mammoth), *Equus* (horse) and *Bison* (bison or buffalo), now extinct in the region (apart from reintroduced bison). Similar values have been calculated by Zimov et al. (2012) for north-eastern Siberia, but it is not clear how far these estimates can be extrapolated to other northern regions, such as that of interior Alaska (i.e., the unglaciated region between the Brooks and Alaska Ranges, Fig. 1).

Conditions at high latitudes such as those of interior Alaska were unusual in the last glacial phase because the megafauna inhabited a biome that now has no modern analogue, often termed the ‘mammoth-steppe’ (Guthrie, 1968; Guthrie, 1982; Williams and Jackson, 2007) or ‘steppe-tundra (Anderson et al. 2004). Paleobotanical records indicate vegetation was dominated by herbs (e.g. *Cyperaceae*, *Poaceae*, *Artemisia* and other forbs), with only a minor component of trees and shrubs (*Larix*, *Betula, Salix;* Anderson et al. 2004; Gaglioti et al., 2011; Willerslev et al., 2014; Zazula et al., 2007). Moreover, the palaeo-geography of Alaska was unusual. During the late-glacial maximum, northern and interior Alaska were biologically isolated from the rest of America until the opening of an inland ice-free corridor between the Laurentide and the Cordilleran ice sheets along the eastern slopes of the Rocky Mountains (Kitchen et al., 2008). The estimated date at which the corridor opened and permitted megaherbivore exchange between interior Alaska and the rest of North America varies between 13.4 ka (Heintzman et al., 2016) and 12.6 ka (Pedersen et al., 2016).

In contrast with the southern part of the continent, in Alaska there appear to have been staggered extinctions similar to those observed in Eurasia (Stuart, 2015), Including an *Equus* species (‘hemione-like’ ass) prior to the last glacial maximum (Guthrie, 2003). The last stage of the LQE in Alaska happened during the Pleistocene-Holocene transition and saw the loss of other species of *Equus* (caballine horses), *Mammuthus*, and *Saiga* (Saiga antelope). Evidence from the North Slope and Fairbanks region has provided an estimate of temporal change in megafaunal abundance in the region around the last stages of the LQE but this is based exclusively on an extensive collection of radiocarbon dated bones (Mann et al., 2013).

The combination of *Sporormiella* records and bone data that we use here promises a more robust estimate of change in animal numbers. Our main aim is to study changes in population size and diversity of megaherbivores in interior Alaska across the final stage of the LQE (i.e. the last extinctions believed to have occurred by about 13 ka, Stuart, 2015). We hypothesise that the faunal loss during the final stage of the LQE in interior Alaska was associated with a sharp reduction in total population size across all megaherbivores, as indicated by *Sporormiella* and changes in vegetation cover. Our objectives are as follows:

1. Identify the timing of the last extinctions by compiling a database including all existing, spatially-explicit, radiocarbon-dated megaherbivore bone remains in the region.
2. Assess if three new *Sporormiella* spore records from interior Alaska have different *Sporormiella* spore accumulation rates before and after the last extinctions (as defined in 1).
3. Examine the temporal sequences of 1 and 2 in relation to increasing dominance of woody vegetation across the Pleistocene-Holocene transition (based on existing dated pollen records) to assess any systematic signs of correlation between megaherbiore abundance and tree cover.

The second aim is to compare records of *Sporormiella* and other obligate dung fungal spores to improve the interpretation of dung fungal spore records in this study and in future studies. *Sporormiella* records have been shown to be informative in their own right but they could be improved by extending identification to a wider range of spore types. Here, our objectives are to:

1. Use a wider range of dung fungal spores, such as *Sordaria* and *Podospora* to assess the added interpretative values of these spore types; and

2. Compare the spore record at two nearby sites to assess the local variation of dung fungal spore records.

MATERIALS AND METHODS

Faunal remains database

Geo-located and radiocarbon-dated megaherbivore bone remains from Alaska and the Yukon dated 25,000 calibrated ^{14}C years BP or younger were compiled from relevant published work (Campos et al., 2010; Guthrie, 2006; Lorenzen et al., 2011; Martindale et al., 2016; Meiri et al., 2013; Mann et al., 2013). This time range was chosen to cover a long period before and after the last stage of the LQE. This database approach provides the most comprehensive knowledge of the past distribution of megaherbivores in the region to date and includes the taxa: *Mammuthus*, *Equus*, *Saiga*, *Bison*, *Alces* (moose or elk in British English), *Ovibos* (muskox), *Rangifer* (caribou, or reindeer in British English) and *Cervus* (elk or red deer in British English). Records of exceptional Holocene survival of *Mammuthus* on St Paul Island (Graham et al., 2016) were excluded.

The dated megaherbivore bone remains are drawn from very large collections of bones made over more than a century, and both the original collecting and the selection of bones for dating were made largely without regard to stratigraphic context, as they were surface finds made opportunistically on river bars and point bluffs (Guthrie, 2006, Mann et al., 2013). In this respect, the dates are a near-random reflection of faunal remain presence or absence in space and time.

Importantly, although species composition changes dramatically, the overall record of bone dates is almost continuous through the study period. In addition, the geographical distribution of bone remains is widespread across Alaska and the western Yukon (Fig. 1A). This supports the assumption that the rise and decline of remains for individual taxa in our database is likely to be a reflection of past population dynamics.

All dates were made on bone or tooth collagen and 95% (519 out of 546) were obtained by Accelerator Mass Spectrometry (AMS) (Supplementary Table 2). Further confidence in the dating is provided by their permafrost and/or anaerobic context, which maximises endogenous collagen preservation and limits diagenesis (Guthrie, 2006, Mann et al., 2013). Although ultrafiltration and hydroxyproline dating can increase accuracy (Kosintsev et al., 2019), even in permafrost-preserved bones (Zazula et al., 2017), this mostly affects specimens dated to >25 ka, beyond the range of the present study. Raw radiocarbon age determinations were calibrated using IntCal13 in OxCal (Reimer et al., 2013) and all ages are presented as thousands of calibrated ^{14}C years before present (ka).

Coring sites, pollen and fungal spores

Four lakes in interior Alaska, Jan Lake, Windmill Lake, Ruppert Lake and Woody Bottom Pond, were cored. Table 1 summarises site characteristics, coring years and original publications for core chronologies, while the location of each lake is mapped in Figure 1. Jan Lake's basin (Fig. 1B) is formed by an alluvium dam from the

Tanana River and its watershed characterised by metamorphic bedrock hills, with no major inlets. The surrounding vegetation is spruce, birch and aspen forest. Windmill Lake (Fig. 1C) lies in a closed moraine-dammed basin with no major inlets. It is surrounded today by open sedge tussock vegetation with willow and nearby birch and spruce. Ruppert Lake (Figs. 1D, 1E) is a kettle lake on a terminal moraine. It has one inlet, one outlet and the surrounding forest is dominated by spruce, aspen, birch and willow. Woody Bottom Pond (Figs. 1E, 1F) is another kettle lake situated in close proximity (about 650m) to Ruppert Lake. It has no inlet and is located in a bowl-shaped depression, surrounded by a well-drained moraine ridge. The lake is fringed by sedges, peat mosses and spruce trees, while the surrounding slopes support shrub birch and aspen. All four lakes are located at similar elevations and have similar surface areas of open water (Fig. 1, Table 1).

To study changes in population size and diversity of megaherbivores (first aim), we counted *Sporormiella* spores and pollen from the same samples. Samples were prepared for pollen analysis from 1cm^3 of wet sediment using a standard method outlined in Moore et al. (1991). Pollen and spores were identified at 400x and 1000x magnification. In order to maximise reliability, we counted a minimum of 300 pollen grains (Willis and Bennett, 2001) and *Sporormiella* spores observed during pollen counting were identified and counted. In order to calculate pollen and spore concentrations and accumulation rates, an exotic marker, i.e. a known number of *Lycopodium annotinum* spores, was added to the samples during the laboratory procedure (Wood and Wilmshurst, 2013). *Lycopodium annotinum* spores tablets were provided by Lund University and the tablet batch number for each sample is included in Supplementary Table 1. Identification of dung fungal spores was based on resources listed in Baker et al. (2013). Figure 2 was created using the programme

C2 v 1.3 (Juggins, 2007) and the R package Beeswarm (Eklund, 2016). At two sites, Ruppert Lake and Woody Bottom Pond, we also extended spore identification to other dung fungal spores (including *Sordaria* and *Podospora*) commonly reported in the literature (e.g. van Geel et al., 2003) (second aim).

RESULTS

Faunal remains database

Records of 546 georeferenced and radiocarbon-dated megaherbivore fossils from Alaska and the Yukon were collated (Fig. 1; Supplementary Table 2). The most numerous megaherbivore genera for the study period (25 ka to present) were *Equus* (n = 108), followed by *Rangifer* (n = 95), *Alces* (n = 93), *Mammuthus* (n = 85), *Cervus* (n = 69), *Bison* (n = 63), *Ovibos* (n = 26) and finally *Saiga* (n = 7). Taken at face value, temporal distribution of dated radiocarbon megaherbivore remains indicates that *Mammuthus* and *Equus* were dominant until about 16-15 ka, when *Bison* and *Cervus* numbers increased (Fig. 2). Following the extinction of *Mammuthus* and *Equus* at about 13 ka, and subsequently during the Holocene, *Alces* was dominant, with *Rangifer* increasing in number from the mid-Holocene. We consider the marked regional turnover of megaherbivore dominant taxa around 13 ka indicating the last stage of the LQE in interior Alaska.

The small proportion of bones dated by gas counting (i.e. pre-AMS) do not affect this result: they comprise pre-15 ka *Equus*, *Bison* and *Mammuthus*, Holocene *Rangifer*, *Alces* and *Ovibos*, and three *Bison* in the range 14-13 ka (Supplementary Table 2). All of these are corroborated by AMS dates on other specimens, and none determines a first or last appearance datum. When plotted chronologically (Fig. 2), the data show that the number of megaherbivore bones recovered in Alaska remained high and relatively constant throughout the period under consideration, despite an important turnover of dominant taxa.

Coring sites, pollen and fungal spore

The stratigraphies and chronologies for the four cores have been published previously (Table 1) and the age-depth models are reproduced in Supplementary Figure 1. The core sediments are described in Supplementary Table 3. The median age and sediment accumulation rates (for each sample analysed for pollen or spore) are presented in Supplementary Table 1.

Ages were calibrated and age-depth models were created using the IntCal13 calibration curve (Reimer et al., 2013) and the R package ‘rbacon’ version 2.3 (Blaauw and Christen, 2011). The models used 21, 9, 11 and 9 AMS radiocarbon dates based as far as possible on macro- and micro-fossils for Jan Lake, Windmill Lake, Ruppert Lake and Wood Bottom Pond, respectively. In addition, a tephra layer related to the Aniakchak Caldera Forming Event II, dated to 3.595 ± 0.004 ka in Greenland ice cores (Denton and Pearce 2008; Pearce et al., 2017), was identified and used to further constrain the models in Ruppert Lake and Woody Bottom Pond (Monteath et al., 2017). Finally, the start of a distinct rise in *Alnus* pollen in a high-resolution pollen record from Ruppert Lake (Higuera et al., 2009) was dated to 7.56 ± 0.050 ka. Because of the very close proximity of the two sites, this pollen-inferred date was transposed to the Woody Bottom Pond and included in the age model.

At the three sites straddling the last stage of the LQE (i.e. Jan Lake, Windmill Lake, Ruppert Lake), the overall abundance of *Sporormiella* does not diminish after the last extinctions at the transition between the late Glacial and the Holocene (Table 2; Fig. 2). Spore values are highly variable and spore accumulation is plotted together with spore abundance relative to the pollen sum in Supplementary Figures 2-5. At these three sites , *Sporormiella* spores occurred in fewer than half the counted samples at Ruppert Lake, but in all samples at Jan Lake and Windmill Lake (Table 2). A total of 208 individual S*porormiella* spores were identified at these sites (20, 131, and 57, respectively). Accumulation rates varied between 0 and 371.6 spores cm^{-2} yr^{-1} (Table 2). Ruppert Lake spore average accumulation values (Table 2) are similar before and after the last extinctions (4.1 vs 3.4 spores cm^{-2} yr^{-1}). At Windmill, after the last extinctions, values are lower than before (70.2 vs 105.5; Table 2); here, pre-LQE higher values pre-dating the last extinctions are mostly driven by a peak of *Sporormiella* accumulation rate occurring near 13 ka (Fig. 2). Jan Lake has high average accumulation rates after the last extinctions (146.0), compared with an average of 70.9 before. At this site, the earliest record may have been derived from terrestrial or very shallow sediments, and thus reflecting differential recruitment of spores to the site (Carlson and Finney, 2004; ME and MvH personal observation). Our fourth site, Woody Bottom Pond, does not span the last stage of the LQE and 30 individual *Sporormiella* spores were counted with an average accumulation rate of 8.4 spores cm^{-2} yr^{-1} over the Holocene.

For the two sites with a more detailed spore analysis, Ruppert Lake and Woody Bottom Pond, the most common fungal spore was *Sordaria* (n = 36; n = 47, respectively), followed by *Sporormiella* (n = 20; n = 39, respectively) with only one occurrence of *Podospora*. At Ruppert Lake, there was a near-significant correlation ($p=0.052$) between *Sporormiella* and *Sordaria* using a Spearman's rank test, while at Woody Bottom Pond this correlation was highly significant ($p<0.001$).

At Ruppert Lake, *Sordaria* shows higher accumulation rates after the last extinctions (average 6.7 spores cm^{-2} yr^{-1}) compared with an average of 2.6 spores cm^{-2} yr^{-1} before. The Holocene record from Woody Bottom Pond has greater average *Sporormiella* accumulation rates than the entire Ruppert Lake record, with an average accumulation rate of 8.4 spores cm^{-2} yr^{-1} (range 0 – 84.3 spores cm^{-2} yr^{-1}). *Sordaria* has an average accumulation rate of 9.2 spores (Table 2). Few spores are recorded in the last ~3000 years of the record and, as at Ruppert Lake, values fluctuate from sample to sample.

At the three sites straddling the last stage of the LQE, pollen of woody taxa rises around 14 ka, signalling the shift from herbaceous vegetation to shrub tundra and then to woodland and boreal forest as a response to deglacial climate change (Anderson et al 2004). There is no correlation between *Sporormiella* abundance and arboreal pollen percentages (Fig. 2).

DISCUSSION

Our main aim was to study changes in the population size and diversity of megaherbivores in interior Alaska at the final stage of the LQE (i.e. the last extinctions believed to have occurred by about 13 ka). We hypothesise that faunal loss at the final stage of the LQE in interior Alaska is associated with a sharp reduction in megaherbivore population size and changes in vegetation cover. Our secondary aim was to investigate the significance of using a wider range of dung fungal spores at two close-by sites to improve the interpretation of dung fungal spore records in this study and in future studies.

At four sites covering different time intervals (Ruppert Lake 17-0 ka, Jan Lake 14.2-4.6 ka, Windmill Lake 14.8-9.8 ka and Woody Bottom Pond, 9.5-0 ka), significant numbers of *Sporormiella* spores occur from 17 ka to the present. Spore numbers and estimated accumulation rates show variability within each core and among sites. This is typical of *Sporormiella* records (e.g. Davis and Shafer, 2006), which are often described informally as a 'noisy' signal. However, the presence of *Sporormiella* in all samples at two of our sites (Windmill Lake and Jan Lake) suggests the continuous presence of megaherbivores into the Holocene. At Ruppert Lake, *Sporormiella* spores were not observed in all samples, which could be interpreted as low numbers (or absence) of megaherbivores visiting the lake. Here, overall *Sporormiella* counts are low when compared with the other sites (Table 2), and it is therefore difficult to assess if these zero-counts represent true absence or if the small quantity falls below the detection limit (e.g. Walanus and Nalepka, 2013). For future investigations, uncertainty regarding *Sporormiella* zero counts could be avoided by more strictly adhering to the guidelines set by Etienne and Jouffroy-Bapicot (2014) recommending high exotic marker counts, independently from pollen sum. We also found that, when *Sordaria*, another reliable indicator of megaherbivores (Baker et al., 2013; Perrotti and van Asperen, 2019) is counted, the number of samples with indicative spores (i.e. *Sporormiella* and/or *Sordaria*) is doubled (12 vs 25 samples of 48 total). Therefore, including other dung fungal spores such as *Sordaria* appears to be an effective additional measure to minimise the uncertainty associated with *Sporormiella* zero counts.

Besides megaherbivore abundance, other factors affect spore abundance (van Asperen et al., 2019). These factors include (1) moisture availability for fungal growth and hydrology (Wood and Wilmshurst, 2011), (2) shoreline morphology, (3) seasonality of climate and wind impacting fungal growth and dispersal (van Asperen, 2017), (4) taphonomic effects including the sedimentary environment and spore preservation, and (5) laboratory procedures (van Asperen et al., 2016). Thus, with each site having unique environmental and sedimentary conditions, there is unlikely to be a direct relationship between the number of dung fungal spores and the abundance of megaherbivores that applies across sites. Despite these caveats, when megaherbivore abundance is driven by a region-wide process, synchronous and local changes in dung fungal spore abundances can be expected at each site.

Comparison of values of spores before and after the last extinctions (Fig. 2) shows that at Ruppert Lake the range of values remained similar, at Jan Lake there was an increase and at Windmill Lake the values remained similar but for a peak at 14-13 ka. From these data, we can conclude that there was no dramatic change in megaherbivore biomass associated with the LQE and the onset of the Holocene at any of the sites, and by extension at the regional level.

At Ruppert Lake, we extended the counting and identification to a wider range of dung fungi, including *Sporormiella*, *Sordaria* and *Podospora*. We also analysed an additional well-dated core from nearby Woody Bottom Pond that spanned most of the Holocene. We found substantial differences between these two sites, but these differences were reduced when accounting for a wider range of dung fungal spores (Fig. 2). Different species of dung fungi have preferences for certain types of dung (e.g. Richardson, 2001, 1972) and demonstrate species-specific responses to different environmental conditions (Dix and Webster, 1995; Krug et al., 2004). Consequently, some taxa may grow better in certain conditions, resulting in spore assemblages dominated by one species or a group of species with similar ecology. Dix and Webster (1995) also highlight the importance of competition between species as a driver for the composition of the dung fungal community. This suggests that dung fungal biomass, and thus ultimately spore production, is strongly limited by factors such as space, nutrient and moisture availability. Therefore, the sum of individual dung spores, and not the types taken individually, may provide the most appropriate proxy for megaherbivore biomass. In fact, we find that some of the apparent randomness in our record can be reduced when considering both *Sporormiella* and *Sordaria* together (Fig. 2).

Even when considering *Sporormiella* and *Sordaria* together, however, Ruppert Lake and Woody Bottom Pond did not show the same temporal pattern of abundance. Although appearing counter-intuitive because these two sites are located close together, this result reinforces earlier findings that the dung fungal spore signal can relate to extremely small spatial scales (e.g. Davies, 2019; Kamerling et al., 2017). This may be explained by the observation of Baker et al. (2016), who found that shore run-off (within <10 m distance from the water) was the most significant process transporting spores into a series of ponds in the Oostvaardersplassen nature reserve, the Netherlands. In the only quantitative dispersal study we are aware of, Gill et al. (2013) demonstrated the importance of short-distance wind dispersal (<100 m) to explain the significant relationship between local bison distribution and spore abundance in the Konza Prairie, Kansas, USA. While the latter was conducted in grasslands, away from wetland depositional environments, both studies indicate key dispersal distances considerably less than the 650 m separating these two lakes. The emerging pattern within these studies and others (e.g. Davies, 2019; Etienne et al., 2013; Raper and Bush, 2009) is that dung fungal spores produce a local, short-distance signal of megaherbivore activity. In a vast region such as interior Alaska there is a need for using as many sites as possible to gain a landscape-wide understanding of megaherbivore distribution and abundance.

Uniquely, we are able to compare spore counts with fossil bone data. During the period leading to the final stage of the LQE, there was a significant taxonomic turnover of dominant megaherbivores in the bone fossil record (Fig. 2). An initial assemblage dominated by *Mammuthus* and *Equus* (and in the late-glacial, *Cervus*) was followed, after a period of transition ending around 13 ka, by an assemblage dominated by *Bison*, *Alces* and, later in the Holocene, by *Rangifer*. The period of transition is characterised by the extinction in North America of three genera (*Mammuthus*, *Equus* and *Saiga*; Stuart, 2015), although *Mammuthus* survived on the Island of St Paul until 5600 years ago (Graham et al., 2016). It appears that most of the extinctions and the period of dominance turnover occurred before the opening of the ice-free corridor, estimated at 13.4 ka (Heintzman et al., 2016) or 12.6 ka (Pedersen et al., 2016). It is unclear how isolation from the rest of North America would have impacted megaherbivore abundance. The lack of North-South exchange in North America may have limited long-distance dispersal, believed to be key to megaherbivore species survival in the region (Mann et al., 2019, 2015). The extinctions associated with the transition around 13 ka seen here represent the final wave of megafauna extinction in the area.

Several records from North America (not Alaska) indicate a causal relationship linking megaherbivore extinctions to subsequent change in forest composition and wildfire regimes (Gill et al., 2009; Perrotti, 2018; Robinson et al., 2005). In interior Alaska our three sites spanning the final stage of the LQE show that the period 15-12 ka features an increase in woody taxa (largely *Salix* and *Betula*; Bigelow and Edwards, 2001; Carlson and Finney, 2004; Higuera et al., 2009). In two out of three instances the increase in arboreal pollen precedes faunal turnover and in none of the three instances major synchronous decline in *Sporormiella* abundance is evident. Spore accumulation rates either increase or remain stationary following the last extinctions. The last extinctions in the bone dataset at about 13 ka actually represents a major taxonomic turnover, but there is no apparent change in total herbivore numerical abundance. Thus, the stability, or even increase, of spore accumulation rates into the Holocene, which might seem unexpected given results from other regions, is in fact consistent with the maintenance of herbivore population size, albeit via a new suite of taxa. The dominant grazers of the Pleistocene, *Mammuthus* and *Equus*, vanished from the record shortly after the vegetation shift and their places are taken primarily by *Alces*, which is a browser, and later by *Rangifer*.

In interior Alaska, a major ecosystem change developed through the Pleistocene-Holocene transition, and as available feeding niches changed, taxa better adapted to woodland conditions became dominant. The Holocene interior climate likely favoured higher plant biomass than that of the Pleistocene, providing the nutrition (largely but not entirely) for browsers (see Guthrie 2003). Our finding of a shift from a predominantly grazing to browsing herbivore guild, following an increase in woody taxa, suggests that megafaunal extinction may be at least partly related to climate-induced vegetation change, at least in this region. Another significant factor to account for when studying megaherbivore abundance in Alaska is the antiquity of human settlement, potentially dating back earlier than 15 ka and the impact these populations had on their environment with activities such as fire and hunting (Vachula et al., 2019). Moreover, megaherbivore abundance may have remained relatively constant due to a complex history of isolation from the rest of North America until about 13 ka, allowing already resident taxa to expand.

CONCLUSION

In North America, the LQE were particularly severe, with 69% of megafauna species becoming extinct, mostly around the time of the Pleistocene-Holocene transition (14-10 ka) (Stuart, 2015). Dramatic megaherbivore abundance losses associated with the final stage of LQE events have been identified using spores of dung fungus *Sporormiella* at sites from North America, and across the globe. However, such studies are lacking from interior Alaska, a region biologically isolated by ice from the rest of North America until about 13 ka. To study changes in population size and diversity of megaherbivores in interior Alaska, we used a combination of radiocarbon-dated bone data and *Sporormiella* records spanning before and after the final stage of the LQE (i.e. the last extinctions believed to have occurred by about 13 ka).

Based on the bone data, we found that there was a major turnover of dominant megaherbivore species around 13 ka attributable to the final stage of the LQE but, taken at face value, the abundance of bone did not markedly change over time. At the three coring sites spanning the final stage of the LQE, the overall abundance of *Sporormiella* spores did not diminish after the last extinctions. Because there were no synchronous decreases in spore abundance across the three sites, there is no indication that megaherbivore abundance was driven by a region-wide process during this period of time.

There did not appear to be any direct correlation between *Sporormiella* abundance and major vegetation change in the region, which saw pollen of woody taxa pollen rise around 14 ka as a response to deglacial climate change. The rise in woody taxa is associated with an increase in bones of browser species such as *Alces* at two out of three of our sites, suggesting important changes in ecosystem function. By the same token, the loss of the grazing taxa *Mammuthus* and *Equus*, and great reduction in *Bison,* may suggest extinction causality, at least in part, due to climate-driven vegetation change. However, our work did not focus on assessing causes of the LQE and other potential drivers of extinction such as ancient human population active in interior Alaska during this period would require consideration in future research.

Spore values show high variability which is dampened when including *Sordaria*, the only other dung fungal spore type found in significant abundance in our study. From a methodological point of view, our results indicate that high counts and the inclusion of *Sordaria* (and any additional spore type reliably indicating megaherbivore) can improve reliability of results when applying the dung fungal spore method. To confirm the turnover and spatial distribution in megaherbivores across the region, future work should also include more sites with spore studies and additional lines of evidence such as ancient sedimentary DNA or other biomarkers preserved in lake sediments.

The significant strength of our approach is the use of two complementary and independent indicators regarding the presence and abundance of megaherbivores in the past, namely radiocarbon-dated bone remains and accumulation rates of dung fungal spores recovered from radiocarbon-dated lake cores. These two congruent lines of evidence based on state-of-the-art methodology (including three *Sporormiella* records and one bone database) make us relatively confident that there was no long-lasting dramatic loss of megaherbivore abundance in interior Alaska around 13 ka associated with the LQE. This new and robust evidence should act as a cautionary tale against the assumption that regional LQE events are systematically associated with megaherbivore biomass crashes, in addition to taxonomic turnovers. The implication is that studying the consequences of the LQE requires thoroughly testing changes in megaherbivore abundance in time, a critical first step we achieved for interior Alaska. Studies of megaherbivore abundance during periods of substantial climate change such as the last stage of the LQE and the onset of the Holocene can provide valuable insight as we attempt to predict changes in biodiversity and ecosystem function that may occur under future climate scenarios.

ACKNOWLEDGEMENTS

This work was funded by NERC; Lakes and the arctic carbon cycle NE/K000306/1. Radiocarbon dating was supported by the NERC Radiocarbon Facility NRCF010001 (allocation numbers 1726.0813 and 1847.1014) and we kindly acknowledge the efforts of Dr Charlotte Bryant. Tony Stuart kindly shared some dates from the Lister/Stuart megafaunal extinctions project (NERC grants GR3/12599 and NE/D003105/1). We thank Dr Xiaomei Xu at the Keck Carbon Cycle AMS Facility, University of California, Irvine, USA for her expertise in low current AMS. We also thank Hannah Laurens, Tom Roland, and Kim Davies for their invaluable help in the field, and Nancy Bigelow and the Alaska Quaternary Center for the loan of equipment. The manuscript was greatly improved by the comments of two anonymous referees, Associate Editor Jeff Pigati and Senior Editor Derek Booth.

REFERENCE LIST

Anderson, P.M., Edwards, M.E., Brubaker, L.B. 2004. Results and paleoclimate implications of 35 years of paleoecological research in Alaska. Pages 427-440 in A. E. Gillespie, S. C. Porter, and B. F. Atwater, editors. *The Quaternary Period in the United States.* Developments in Quaternary Science. Elsevier, New York.

Baker, A.G., Bhagwat, S.A., Willis, K.J., 2013. Do dung fungal spores make a good proxy for past distribution of large herbivores? Quat. Sci. Rev. 62, 21–31.

Baker, A.G., Cornelissen, P., Bhagwat, S.A., Vera, F.W.M., Willis, K.J., 2016. Quantification of population sizes of large herbivores and their long-term functional role in ecosystems using dung fungal spores. Methods Ecol. Evol. 7, 1273–1281. https://doi.org/10.1111/2041-210X.12580

Bigelow, N.H., Edwards, M.E., 2001. A 14,000 yr paleoenvironmental record from Windmill Lake, central Alaska: Lateglacial and Holocene vegetation in the Alaska range. Quat. Sci. Rev. 20, 203–215. https://doi.org/10.1016/S0277-3791(00)00122-0

Blaauw, M., Christen, J.A., 2011. Flexible paleoclimate age-depth models using an autoregressive gamma process. Bayesian Analysis 6, 457–474.

Bradshaw, R.H.W., Hannon, G.E., Lister, A.M., 2003. A long-term perspective on ungulate–vegetation interactions. For. Ecol. Manage. 181, 267–280. https://doi.org/10.1016/S0378-1127(03)00138-5

Broughton, J.M., Weitzel, E.M., 2018. Population reconstructions for humans and megafauna suggest mixed causes for North American Pleistocene extinctions. Nat. Commun. 9, 1–12. https://doi.org/10.1038/s41467-018-07897-1

Campos, P.F., Willerslev, E., Sher, A., Orlando, L., Axelsson, E., Tikhonov, A., Aaris-Sorensen, K., Greenwood, A.D., Kahlke, R.-D., Kosintsev, P., Krakhmalnaya, T., Kuznetsova, T., Lemey, P., MacPhee, R., Norris, C.A., Shepherd, K., Suchard, M.A., Zazula, G.D., Shapiro, B., Gilbert, M.T.P., 2010. Ancient DNA analyses exclude humans as the driving force behind late Pleistocene musk ox (Ovibos moschatus) population dynamics. Proc. Natl. Acad. Sci. 107, 5675–5680. https://doi.org/10.1073/pnas.0907189107

Carlson, L.J., Finney, B.P., 2004. A 13 000-year history of vegetation and environmental change at Jan Lake, east-central Alaska. Holocene 14, 818–827. https://doi.org/10.1191/0959683604hl762rp

Davis, O.K., Shafer, D.S., 2006. Sporormiella fungal spores, a palynological means of detecting herbivore density. Palaeogeogr. Palaeoclimatol. Palaeoecol. 237, 40–50.

Davies, A.L. 2019. Dung fungi as an indicator of large herbivore dynamics in peatlands. Review of Palaeobotany and Palynology 271, 1-11.

Denton, J.S., Pearce, N.J.G., 2008. Comment on “A synchronized dating of three Greenland ice cores through the Holocene” by B.M. Vinther et al.: no Minoan tephra in the 1642 B.C. layer of the GRIP ice core. Journal of Geophysical Research 113, D04303. http://dx.doi.org/10.1029/2007JD008970

Dix, N.J., Webster, J., 1995. Fungal ecology. Chapman & Hall, London, UK.

Doughty, C.E., Wolf, A., Malhi, Y., 2013. The legacy of the Pleistocene megafauna extinctions on nutrient availability in Amazonia. Nat. Geosci. 6, 1–5. https://doi.org/10.1038/ngeo1895

Edwards, M.E., Barker, E.D., 1994. Climate and vegetation in northeastern Alaska 18,000 yr B.P.-present. Palaeogeogr. Palaeoclimatol. Palaeoecol. 109, 127–135. https://doi.org/10.1016/0031-0182(94)90172-4

Eklund, A., 2016. Package ‘ beeswarm .’

Etienne, D., Jouffroy-Bapicot, I., 2014. Optimal counting limit for fungal spore abundance estimation using Sporormiella as a case study. Veg. Hist. Archaeobot. 23, 743–749. https://doi.org/10.1007/s00334-014-0439-1

Etienne, D., Wilhelm, B., Sabatier, P., 2013. Influence of sample location and livestock numbers on Sporormiella concentrations and accumulation rates in surface sediments of Lake Allos, French Alps. J. Paleolimnol. 49, 117–127. https://doi.org/10.1007/s10933-012-9646-x

Gaglioti, B. V, Barnes, B.M., Zazula, G.D., Beaudoin, A.B., Wooller, M.J., 2011. Late Pleistocene paleoecology of arctic ground squirrel (Urocitellus parryii) caches and nests from Interior Alaska’s mammoth steppe ecosystem, USA. Quat. Res. 76, 373–382. https://doi.org/10.1016/j.yqres.2011.08.004

Galetti, M., Moleón, M., Jordano, P., Pires, M.M., Guimarães, P.R., Pape, T., Nichols, E., Hansen, D., Olesen, J.M., Munk, M., de Mattos, J.S., Schweiger, A.H., Owen-Smith, N., Johnson, C.N., Marquis, R.J., Svenning, J.C., 2018. Ecological and evolutionary legacy of megafauna extinctions. Biol. Rev. 93, 845–862. https://doi.org/10.1111/brv.12374

Gill, J.L., 2014. Ecological impacts of the late Quaternary megaherbivore extinctions. New Phytol. 201, 1163–1169. https://doi.org/10.1111/nph.12576

Gill, J.L., Mclauchlan, K.K., Skibbe, A.M., Goring, S., Zirbel, C.R., Williams, J.W., 2013. Linking abundances of the dung fungus sporormiella to the density of bison: Implications for assessing grazing by megaherbivores in palaeorecords. J. Ecol. 101, 1125–1136. https://doi.org/10.1111/1365-2745.12130

Gill, J.L., Williams, J.W., Jackson, S.T., Lininger, K.B., Robinson, G.S., 2009. Pleistocene megafaunal collapse, novel plant communities, and enhanced fire regimes in North America. Science 326, 1100–3. https://doi.org/10.1126/science.1179504

Graham, R.W., Belmecheri, S., Choy, K., Culleton, B.J., Davies, L.J., Froese, D., Heintzman, P.D., Hritz, C., Kapp, J.D., Newsom, L.A., Rawcliffe, R., Saulnier-Talbot, É., Shapiro, B., Wang, Y., Williams, J.W., Wooller, M.J., 2016. Timing and causes of mid-Holocene mammoth extinction on St. Paul Island, Alaska. Proc. Natl. Acad. Sci. 113, 9310–9314. https://doi.org/10.1073/pnas.1604903113

Guthrie, R. D. 1968. Paleoecology of the large-mammal community in interior Alaska during the late Pleistocene. American Midlands Naturalist 79, 346-363

Guthrie, R.D., 2006. New carbon dates link climatic change with human colonization and Pleistocene extinctions. Nature 441, 207–209. https://doi.org/10.1038/nature04604

Guthrie, R.D., 2003. Rapid body size decline in Alaskan Pleistocene horses before extinction. Nature

426, 169–171. https://doi.org/10.1038/nature02098

Haile, J., Froese, D.G., MacPhee, R.D.E., Roberts, R.G., Arnold, L.J., Reyes, A. V, Rasmussen, M., Nielsen, R., Brook, B.W., Robinson, S., Demuro, M., Gilbert, M.T.P., Munch, K., Austin, J.J., Cooper, A., Barnes, I., Moller, P., Willerslev, E., 2009. Ancient DNA reveals late survival of mammoth and horse in interior Alaska. Proc. Natl. Acad. Sci. U. S. A. 106, 22352–22357.

Heintzman, P.D., Froese, D., Ives, J.W., Soares, A.E.R., Zazula, G.D., Letts, B., Andrews, T.D., Driver, J.C., Hall, E., Hare, P.G., Jass, C.N., MacKay, G., Southon, J.R., Stiller, M., Woywitka, R., Suchard, M.A., Shapiro, B., 2016. Bison phylogeography constrains dispersal and viability of the Ice Free Corridor in western Canada. Proc. Natl. Acad. Sci. 113, 8057–8063. https://doi.org/10.1073/pnas.1601077113

Hempson, G.P., Archibald, S., Bond, W.J., Ellis, R.P., Grant, C.C., Kruger, F.J., Kruger, L.M., Moxley, C., Owen-Smith, N., Peel, M.J.S., Smit, I.P.J., Vickers, K.J., 2015. Ecology of grazing lawns in Africa. Biol. Rev. 90, 979–994. https://doi.org/10.1111/brv.12145

Higuera, P.E., Brubaker, L.B., Anderson, P.M., Hu, F.S., Brown, T.A., 2009. Vegetation mediated the impacts of postglacial climate change on fire regimes in the south-central Brooks Range, Alaska. Ecol. Monogr. 79, 201–219. https://doi.org/10.1890/07-2019.1

Johnson, C.N., 2009. Ecological consequences of Late Quaternary extinctions of megafauna. Proc. Biol. Sci. 276, 2509–19. https://doi.org/10.1098/rspb.2008.1921

Johnson, C.N., Rule, S., Haberle, S.G., Turney, C.S.M., Kershaw, A.P., Brook, B.W., 2015. Using dung fungi to interpret decline and extinction of megaherbivores: problems and solutions. Quat. Sci. Rev. 110, 107–113. https://doi.org/10.1016/j.quascirev.2014.12.011

Juggins, S., 2007. C2 User guide Version 1.5.

Kamerling, I.M., Schofield, J.E., Edwards, K.J., Aronsson, K.Å., 2017. High-resolution palynology reveals the land use history of a Sami renvall in northern Sweden. Veg. Hist. Archaeobot. 26, 369–388. https://doi.org/10.1007/s00334-016-0596-5

Kitchen, A., Miyamoto, M.M., Mulligan, C.J., 2008. A three-stage colonization model for the peopling of the Americas. PLoS One 3. https://doi.org/10.1371/journal.pone.0001596

Koch, P.L., Barnosky, A.D., 2006. Late Quaternary Extinctions: State of the Debate. Annu. Rev. Ecol. Evol. Syst. 37, 215–250. https://doi.org/10.1146/annurev.ecolsys.34.011802.132415

Kosintsev, P., Mitchell, K.J., Devièse, T., van der Plicht, J., Kuitems, M., Petrova, E., Tikhonov, A., Higham, T., Comeskey, D., Turney, C., Cooper, A., van Kolfschoten, T., Stuart, A.J., Lister, A.M. 2019. Evolution and extinction of the giant rhinoceros Elasmotherium sibiricum sheds light on late Quaternary megafaunal extinctions. Nature Ecology and Evolution 3, 31-38.

Krug, J.C., Benny, G.L., Keller, H.W., 2004. Coprophilous fungi, in: Mueller, G.M., Bills, G.F., Foster, M.S. (Eds.), Biodiversity of Fungi. Elsevier, Amsterdam, pp. 468–499.

Lorenzen, E.D., Nogués-Bravo, D., Orlando, L., Weinstock, J., Binladen, J., Marske, K. a, Ugan, A., Borregaard, M.K., Gilbert, M.T.P., Nielsen, R., Ho, S.Y.W., Goebel, T., Graf, K.E., Byers, D., Stenderup, J.T., Rasmussen, M., Campos, P.F., Leonard, J. a, Koepfli, K.-P., Froese, D., Zazula, G., Stafford, T.W., Aaris-Sørensen, K., Batra, P., Haywood, A.M., Singarayer, J.S., Valdes, P.J., Boeskorov, G., Burns, J. a, Davydov, S.P., Haile, J., Jenkins, D.L., Kosintsev, P., Kuznetsova, T., Lai, X., Martin, L.D., McDonald, H.G., Mol, D., Meldgaard, M., Munch, K., Stephan, E., Sablin, M., Sommer, R.S., Sipko, T., Scott, E., Suchard, M. a, Tikhonov, A.N., Willerslev, R., Wayne, R.K., Cooper, A., Hofreiter, M., Sher, A., Shapiro, B., Rahbek, C., Willerslev, E., 2011. Species-specific responses of Late Quaternary megafauna to climate and humans. Nature 479, 359–64. https://doi.org/10.1038/nature10574

Malhi, Y., Doughty, C.E., Galetti, M., Smith, F.A., Svenning, J., Terborgh, J.W., 2016. Megafauna and ecosystem function from the Pleistocene to the Anthropocene. Proc. Natl. Acad. Sci. 113, 838–846. https://doi.org/10.1073/pnas.1502540113

Mann, D.H., Groves, P., Gaglioti, B. V, Shapiro, B.A., 2019. Climate-driven ecological stability as a globally shared cause of Late Quaternary megafaunal extinctions: the Plaids and Stripes Hypothesis. Biol. Rev. 94, 328–352. https://doi.org/10.1111/brv.12456

Mann, D.H., Groves, P., Kunz, M.L., Reanier, R.E., Gaglioti, B. V, 2013. Ice-age megafauna in Arctic Alaska: Extinction, invasion, survival. Quat. Sci. Rev. 70, 91–108. https://doi.org/10.1016/j.quascirev.2013.03.015

Mann, D.H., Groves, P., Reanier, R.E., Gaglioti, B. V, Kunz, M.L., Shapiro, B., 2015. Life and extinction of megafauna in the ice-age Arctic. Proc. Natl. Acad. Sci. 112, 14301–14306. https://doi.org/10.1073/pnas.1516573112

Martindale, A., Morlan, R., Betts, M., Blake, M., Gajewski, K., Chaput, M., Mason, A., Vermeersch, P., 2016. Canadian Archaeological Radiocarbon Database (CARD 2.1) [WWW Document]. URL http://www.canadianarchaeology.ca/ (accessed 11.1.16).

McGowan, S., Anderson, N.J., Edwards, M.E., Hopla, E., Jones, V., Langdon, P.G., Law, A., Soloveiva, N., Turner, S., van Hardenbroek, M., Whiteford, E.J., Wiik, E., 2018. Vegetation transitions drive the autotrophy-heterotrophy balance in Arctic lakes. Limnol. Oceanogr. Lett. 3, 246–255. https://doi.org/10.1002/lol2.10086

Meiri, M., Lister, A.M., Collins, M.J., Tuross, N., Goebel, T., Blockley, S., Zazula, G.D., van Doorn, N., Guthrie, R.D., Boeskorov, G.G., Baryshnikov, G.F., Sher, A., Barnes, I., 2013. Faunal record identifies Bering isthmus conditions as constraint to end-Pleistocene migration to the New World. Proc. R. Soc. B Biol. Sci. 281. https://doi.org/10.1098/rspb.2013.2167

Monteath, A. J., van Hardenbroek, M., Davies, L. J., Froese, D. G., Langdon, P. G., Xu, X., Edwards, M. E. 2017. Chronology and glass chemistry of tephra and cryptotephra horizons from lake sediments in northern Alaska, USA. Quat. Res. 88, 169-178.

Moore, P.D., Webb, J.A., Collison, M.E., 1991. Pollen analysis. Blackwell Scientific Publications.

Pearce, C., Varhelyi, A., Wastegård, S., Muschitiello, F., Barrientos, N., O'Regan, M., Cronin, T., et al. 2016. The 3.6 ka Aniakchak tephra in the Arctic Ocean: a constraint on the Holocene radiocarbon reservoir age in the Chukchi Sea. Climate of the Past Discussions (in review). http://dx.doi.org/10.5194/cp-2016-112.

Pedersen, M.W., Ruter, A., Schweger, C., Friebe, H., Staff, R.A., Kjeldsen, K.K., Mendoza, M.L.Z., Beaudoin, A.B., Zutter, C., Larsen, N.K., Potter, B.A., Nielsen, R., Rainville, R.A., Orlando, L., Meltzer, D.J., Kjær, K.H., Willerslev, E., 2016. Postglacial viability and colonization in North America's ice-free corridor. Nature 537, 45–49. https://doi.org/10.1038/nature19085

Peres, C.A., Emilio, T., Schietti, J., Desmoulière, S.J.M., Levi, T., 2016. Dispersal limitation induces long-term biomass collapse in overhunted Amazonian forests. Proc. Natl. Acad. Sci. 113, 892–897. https://doi.org/10.1073/pnas.1516525113

Perrotti, A.G., 2018. Pollen and Sporormiella evidence for terminal Pleistocene vegetation change and megafaunal extinction at Page-Ladson, Florida. Quat. Int. 466, 256–268. https://doi.org/10.1016/j.quaint.2017.10.015

Perrotti, A.G., van Asperen, E., 2019. Dung fungi as a proxy for megaherbivores: opportunities and limitations for archaeological applications. Veg. Hist. Archaeobot. https://doi.org/10.1007/s00334-018-0686-7

Rabanus-Wallace, M.T., Wooller, M.J., Zazula, G.D., Shute, E., Jahren, A.H., Kosintsev, P., Burns, J.A., Breen, J., Llamas, B., Cooper, A., 2017. Megafaunal isotopes reveal role of increased moisture on rangeland during late Pleistocene extinctions. Nat. Ecol. Evol. 1. https://doi.org/10.1038/s41559-017-0125

Raper, D., Bush, M., 2009. A test of Sporormiella representation as a predictor of megaherbivore presence and abundance. Quat. Res. 71, 490–496.

Reimer, P.J., Bard, E., Bayliss, A., Beck, J.W., Blackwell, P.G., Ramsey, C.B., Buck, C.E., Cheng, H., Edwards, R.L., Friedrich, M., Grootes, P.M., Guilderson, T.P., Haflidason, H., Hajdas, I., Hatté, C., Heaton, T.J., Hoffmann, D.L., Hogg, A.G., Hughen, K.A., Kaiser, K.F., Kromer, B., Manning, S.W., Niu, M., Reimer, R.W., Richards, D.A., Scott, E.M., Southon, J.R., Staff, R.A., Turney, C.S.M., van der Plicht, J., 2013. IntCal13 and Marine13 Radiocarbon Age Calibration Curves 0–50,000 Years cal BP. Radiocarbon 55, 1869–1887. https://doi.org/10.2458/azu_js_rc.55.16947

Richardson, M.J., 2001. Diversity and occurrence of coprophilous fungi. Mycol. Res. 105, 387–402.

Richardson, M.J.M.J., 1972. Coprophilous ascomycetes on different dung types. Trans. Br. Mycol. Soc. 58, 37–48. https://doi.org/10.1016/S0007-1536(72)80069-X

Robinson, G.S., Burney, L.P., Burney, D.A., 2005. Landscape paleoecology and megafaunal extinction in southeastern New York state. Ecol. Monogr. 75, 295–315.

Sandom, C.J., Ejrnaes, R., Hansen, M.D.D., Svenning, J.-C., 2014. High herbivore density associated with vegetation diversity in interglacial ecosystems. Proc. Natl. Acad. Sci. 1–6. https://doi.org/10.1073/pnas.1311014111

Stuart, A.J., 2015. Late Quaternary megafaunal extinctions on the continents: a short review. Geol. J. 338–363. https://doi.org/10.1002/gj

Vachula, R.S., Huang, Y., Longo, W.M., Dee, S.G., Daniels, W.C., Russell, J.M. 2019. Evidence of Ice Age humans in eastern Beringia suggests early migration to North America. Quat. Sci. Rev. 205, 35-44.

van Asperen, E.N., 2017. Fungal diversity on dung of tropical animals in temperate environments: Implications for reconstructing past megafaunal populations. Fungal Ecol. 28, 25–32. https://doi.org/10.1016/j.funeco.2016.12.006

van Asperen, E.N., Kirby, J.R., Hunt, C.O., 2016. The effect of preparation methods on dung fungal spores: Implications for recognition of megafaunal populations. Rev. Palaeobot. Palynol. 229, 1–8. https://doi.org/10.1016/j.revpalbo.2016.02.004

Van Asperen, E.N., Kirby, J.R., Shaw, H.E. 2019. Relating dung fungal spore influx rates to animal density in a temperate environment: Implications for palaeoecological studies. The Holocene. 0, 1-15. https://doi.org/10.1177/0959683619875804

van Geel, B., Buurman, J., Brinkkemper, O., Schelvis, J., Aptroot, A., van Reenen, G.B.A., Hakbijl, T., 2003. Environmental reconstruction of a Roman Period settlement site in Uitgeest (The Netherlands), with special reference to coprophilous fungi. J. Archaeol. Sci. 30, 873–883.

Walanus, A., Nalepka, D., 2013. Information content of zero pollen counts in Holocene profiles. The Holocene 23, 732–738. https://doi.org/10.1177/0959683612465444

Willerslev, E., Davison, J., Moora, M., Zobel, M., Coissac, E., Edwards, M.E., Lorenzen, E.D., Vestergård, M., Gussarova, G., Haile, J., Craine, J., Gielly, L., Boessenkool, S., Epp, L.S., Pearman, P.B., Cheddadi, R., Murray, D., Bråthen, K.A., Yoccoz, N., Binney, H., Cruaud, C., Wincker, P., Goslar, T., Alsos, I.G., Bellemain, E., Brysting, A.K., Elven, R., Sønstebø, J.H., Murton, J., Sher, A., Rasmussen, M., Rønn, R., Mourier, T., Cooper, A., Austin, J., Möller, P., Froese, D., Zazula, G., Pompanon, F., Rioux, D., Niderkorn, V., Tikhonov, A., Savvinov, G., Roberts, R.G., MacPhee, R.D.E., Gilbert, M.T.P., Kjær, K.H., Orlando, L., Brochmann, C., Taberlet, P., 2014. Fifty thousand years of Arctic vegetation and megafaunal diet. Nature 506, 47–51. https://doi.org/10.1038/nature12921

Williams, J.W., Jackson, S.T., 2007. Novel climates, no-analog communities, and ecological surprises. Front. Ecol. Environ. 5, 475–482. https://doi.org/10.1890/070037

Willis, K.J., Bennett, K.D., 2001. Pollen, in: Smol, J.P., Birks, H.J.B., Last, W.M. (Eds.), Tracking Environmental Change Using Lake Sediments Volume 3 Terrestrial, Algal and Siliceous Indicators. Kluwer Academic Publishers, Dordrecht, pp. 5–32.

Wood, J.R., Wilmshurst, J.M., 2013. Accumulation rates or percentages? How to quantify Sporormiella and other coprophilous fungal spores to detect late Quaternary megafaunal extinction events. Quat. Sci. Rev. 77, 1–3. https://doi.org/10.1016/j.quascirev.2013.06.025

Wood, J.R., Wilmshurst, J.M., 2011. Wetland soil moisture complicates the use of Sporormiella to trace past herbivore populations. J. Quat. Sci. 27, 254–259. https://doi.org/10.1002/jqs.1539

Zazula, G.D., Froese, D.G., Elias, S.A., Kuzmina, S., Mathewes, R.W., 2007. Arctic ground squirrels of the mammoth-steppe: paleoecology of Late Pleistocene middens (~24 000-29 450 14C yr BP), Yukon Territory, Canada. Quat. Sci. Rev. 26, 979–1003. https://doi.org/10.1016/j.quascirev.2006.12.006

Zazula, G.D., MacPhee, R.D.E., Southon, J., Nalawade-Chavan, S., Reyes, A.V., Hewitson, S., Hall, E. 2017. A case of early Wisconsin “over-chill”: new radiocarbon evidence for early extirpation of western camel (Camelops hesternus) in eastern Beringia. Quat. Sci. Rev. 171, 48-57.

Zimov, S.A., Zimov, N.S., Tikhonov, A.N., Chapin, F.S., 2012. Mammoth steppe: a high-productivity phenomenon. Quat. Sci. Rev. 57, 26–45. https://doi.org/10.1016/j.quascirev.2012.10.005

Figures and tables

Table 1: Characteristics of the lake study sites

	New Data (this paper)	Surface area (ha)	Water depth (m)	Altitude (m asl)	Latitude (N)	Longitude (W)	Year cored	Core Chronology
Jan Lake	*Sporormiella*	10.1	11.7	503	63.57	142.90	1994	Carlson and Finney, 2004
Windmill Lake	*Sporormiella*	2.0	4	630	63.65	148.80	1994	Bigelow and Edwards 2001; Carlson and Finney, 2004
Ruppert Lake	All fungal spores	4.9	5.8	230	67.07	154.24	2013	Monteath et al. 2017; McGowan et al. 2018
Woody Bottom Pond	All fungal spores	0.7	4.3	310	67.07	154.23	2013	Monteath et al. 2017; McGowan et al. 2018

Table 2: Summary of spore counts. Note that total dung fungal spore counts in Ruppert Lake includes one *Podospora* spore, in addition to *Sordaria* and *Sporormiella* spores.

	Jan Lake	Windmill Lake	Ruppert Lake	Woody Bottom Pond
Age range (ka)	14.2 - 4.6	14.8 - 9.5	17 - 0	9.5 - 0
Total *Sporormiella* spores counted	131	57	20	39
Frequency of *Sporomiella* occurrence relative to all samples	20 out of 20	11 out of 11	12 out of 48	17 out of 45
Pre-LQE *Sporomiella* average accumulation rates, range between parentheses (spores cm^{-2} yr^{-1}).	70.9 (57.3 - 90.4)	105.5 (31.5 - 212.9)	4.1 (0 - 39.0)	n/a
Post-LQE *Sporomiella* average accumulation rates, range between parentheses (spores cm^{-2} yr^{-1}).	146.0 (11.5 – 371.6)	70.2 (41.1 – 113.7)	3.4 (0 -25.7)	8.4 (0 - 84.3)
Total *Sordaria* spores counted			36	47
Frequency of *Sordaria* occurrence relative to all samples			17 out of 48	15 out of 45
Pre-LQE *Sordaria* average accumulation rates, range between parentheses (spores cm^{-2} yr^{-1}).			2.6 (0 – 35.5)	n/a
Post-LQE *Sordaria* average accumulation rates, range between parentheses (spores cm^{-2} yr^{-1}).			6.7 (0 -46.0)	9.2 (0 – 77.8)
Total dung spores counted			57	86
Frequency of dung spores occurrence relative to all samples			25 out of 48	22 out of 45
Pre-LQE dung spores average accumulation rates, range between parentheses (spores cm^{-2} yr^{-1}).			6.6 (0 - 39.0)	n/a
Post-LQE dung spores average accumulation rates, range between parentheses (spores cm^{-2} yr^{-1}).			13.1 (0 - 56.5)	8.4 (0 - 84.3)

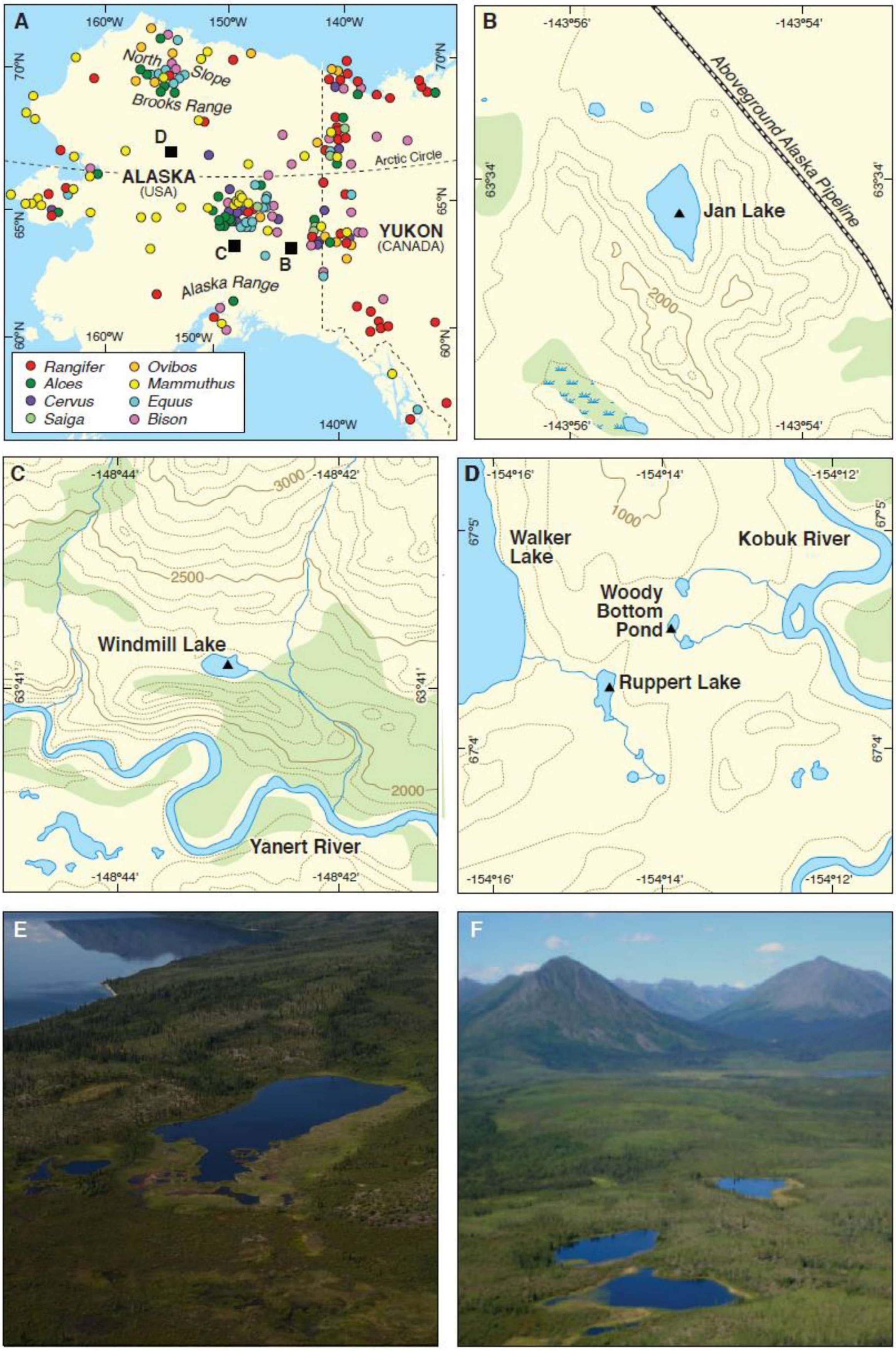
A
160°W
150°W
140°W
70°N
65°N
60°N
North Slope
Brooks Range
D
ALASKA
(USA)
Arctic Circle
C
B
YUKON
(CANADA)
Alaska Range
Rangifer
Alces
Cervus
Saiga
Ovibos
Mammuthus
Equus
Bison
B
-143°56'
-143°54'
63°34'
Aboveground Alaska Pipeline
Jan Lake
2000
C
-148°44'
-148°42'
3000
2500
Windmill Lake
63°41'
2000
Yanert River
D
-154°16'
-154°14'
-154°12'
67°5'
67°4'
1000
Walker Lake
Kobuk River
Woody Bottom Pond
Ruppert Lake
E
F

Figure 1. Location of bone remains and lake sites. A: Map of Alaska locating megaherbivore bone remains 25 ka or younger (circles, see source publication in methods and Supplementary Table 2) and lake sites (squares). B. Jan Lake, an alluvium-dammed basin with spore and pollen record spanning 14.2-4.6 ka. C. Windmill Lake, a moraine-dammed basin with spore and pollen record spanning 14.8-9.5 ka. D. Ruppert Lake and Woody Bottom Pond, two kettle lakes with spore and pollen records spanning 17-0 ka and 9.5-0 ka, respectively. E. Oblique aerial photograph of Ruppert Lake with the larger Walker Lake, top left (photo by Tom Roland). F. Oblique aerial photograph of Woody Bottom Pond (middle lake, photo by Maarten van Hardenbroek). Altitude is reported in feet.

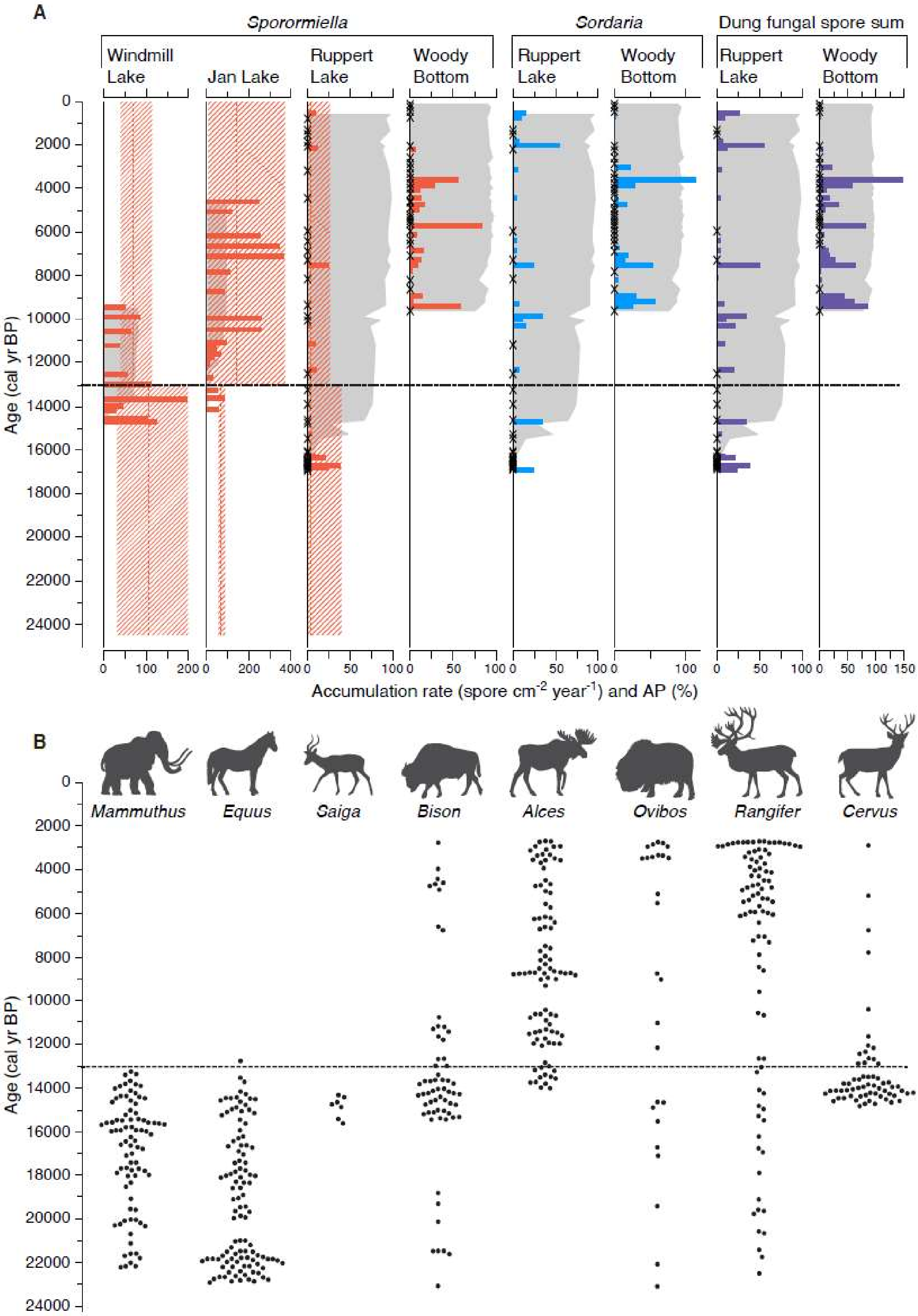
A
Sporormiella
Sordaria
Dung fungal spore sum
Windmill Lake
Jan Lake
Ruppert Lake
Woody Bottom
Ruppert Lake
Woody Bottom
Ruppert Lake
Woody Bottom
Age (cal yr BP)
0
2000
4000
6000
8000
10000
12000
14000
16000
18000
20000
22000
24000
0 100 200
0 200 400
0 50 100
0 50 100
0 50 100
0 100
0 50 100
0 50 100 150
Accumulation rate (spore cm^{-2} year^{-1}) and AP (%)
B
Mammuthus
Equus
Saiga
Bison
Alces
Ovibos
Rangifer
Cervus
Age (cal yr BP)
0
2000
4000
6000
8000
10000
12000
14000
16000
18000
20000
22000
24000

Figure 2. Spore and bone diagram. A. Dung fungal spore accumulation rates (spore per cm^2 per year) are shown as coloured bars and percent arboreal pollen (%AP) is shown as grey shading. The mean and range of spore accumulation rates before and after the last extinctions is indicated with a dotted line and hashed zones, respectively. A small cross indicates samples where no dung fungal spores were encountered. B. Megaherbivore bone remains 25 ka or younger from Alaska, plotted against time. Each bone is plotted as a dot using the median calibrated radiocarbon date.

Figure 1

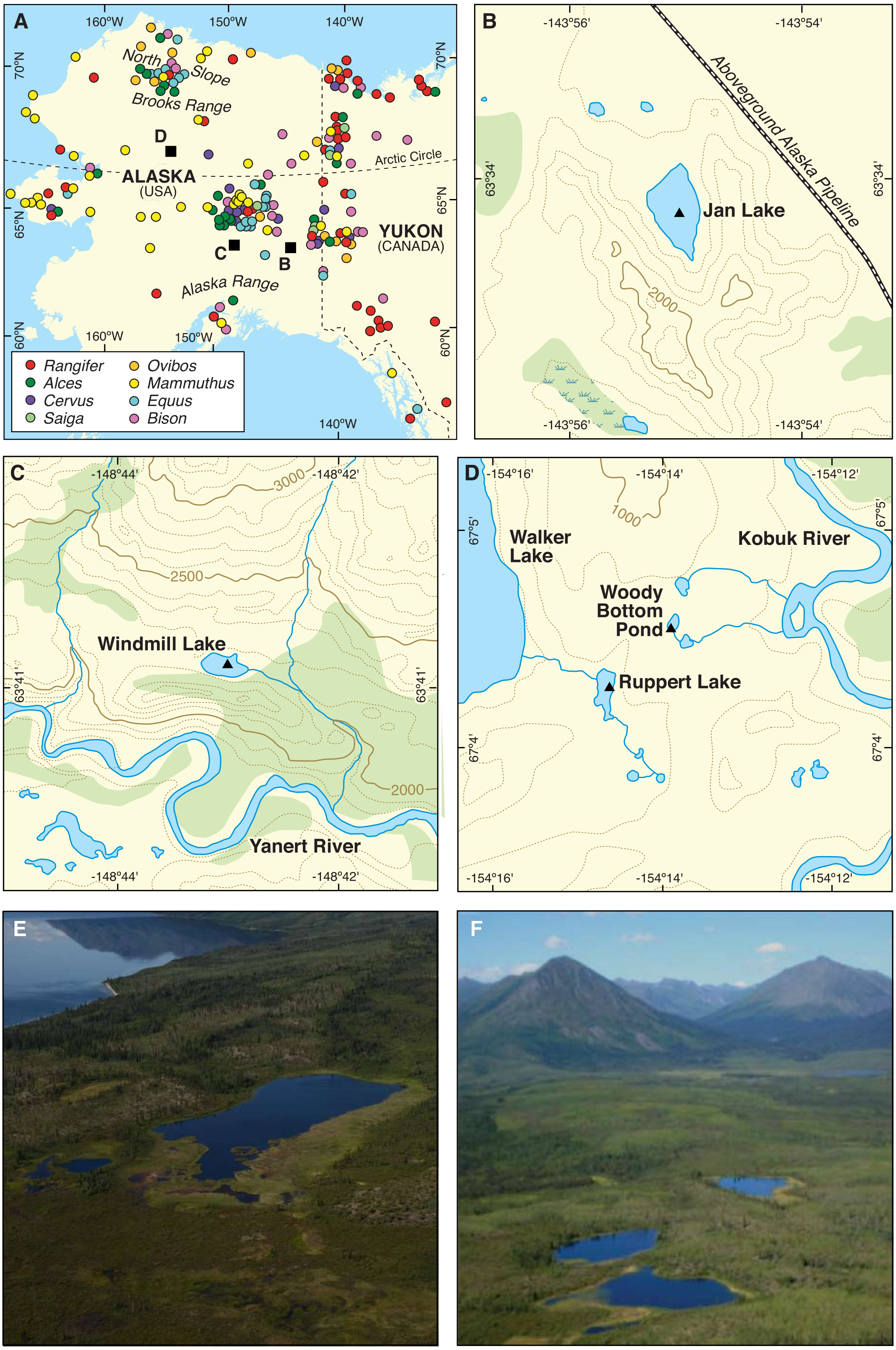
A
160°W
150°W
140°W
70°N
65°N
60°N
North Slope
Brooks Range
D
ALASKA
(USA)
Arctic Circle
C
B
YUKON
(CANADA)
Alaska Range
160°W
150°W
140°W
Rangifer
Alces
Cervus
Saiga
Ovibos
Mammuthus
Equus
Bison
B
-143°56'
-143°54'
63°34'
Aboveground Alaska Pipeline
Jan Lake
2000
C
-148°44'
-148°42'
3000
2500
Windmill Lake
63°41'
2000
Yanert River
D
-154°16'
-154°14'
-154°12'
67°5'
Walker Lake
1000
Kobuk River
Woody Bottom Pond
Ruppert Lake
67°4'
E
F

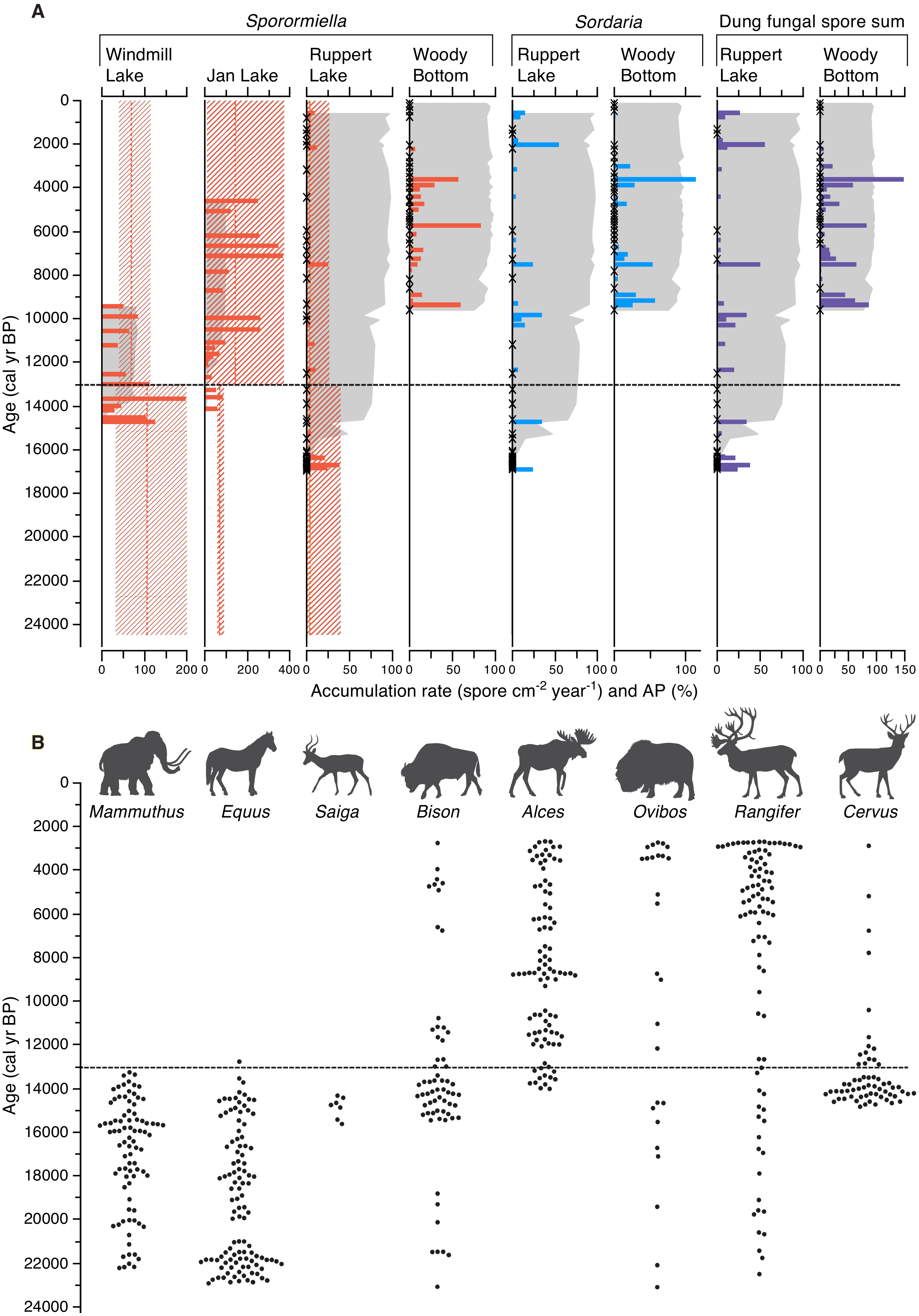
A
Sporormiella
Windmill Lake
Jan Lake
Ruppert Lake
Woody Bottom
Sordaria
Ruppert Lake
Woody Bottom
Dung fungal spore sum
Ruppert Lake
Woody Bottom
Age (cal yr BP)
0
2000
4000
6000
8000
10000
12000
14000
16000
18000
20000
22000
24000
0 100 200
0 200 400
0 50 100
0 50 100
0 50 100
0 100
0 50 100
0 50 100 150
Accumulation rate (spore cm^{-2} year^{-1}) and AP (%)
B
Mammuthus
Equus
Saiga
Bison
Alces
Ovibos
Rangifer
Cervus
Age (cal yr BP)
0
2000
4000
6000
8000
10000
12000
14000
16000
18000
20000
22000
24000

Table 1 and 2

	New Data (this paper)	Surface area (ha)	Water depth (m)	Altitude (m asl)	Latitude (N)	Longitude (W)	Year cored
Jan Lake	*Sporormiella*	10.1	11.7	503	63.57	142.90	1994
Windmill Lake	*Sporormiella*	2.0	4	630	63.65	148.80	1994
Ruppert Lake	All fungal spores	4.9	5.8	230	67.07	154.24	2013
Woody Bottom Pond	All fungal spores	0.7	4.3	310	67.07	154.23	2013

Core Chronology
Carlson and Finney, 2004
Bigelow and Edwards 2001; Carlson and Finney, 2004
Monteath et al. 2017; McGowan et al. 2018
Monteath et al. 2017; McGowan et al. 2018

	Jan Lake	Windmill Lake
Age range (ka)	14.2 - 4.6	14.8 - 9.5
Total *Sporormiella* spores counted	131	57
Frequency of *Sporomiella* occurrence relative to all samples	20 out of 20	11 out of 11
Pre-LQE *Sporomiella* average accumulation rates, range between parentheses (spores cm^{-2} yr^{-1}).	70.9 (57.3 - 90.4)	105.5 (31.5 - 212.9)
Post-LQE *Sporomiella* average accumulation rates, range between parentheses (spores cm^{-2} yr^{-1}).	146.0 (11.5 – 371.6)	70.2 (41.1 – 113.7)
Total *Sordaria* spores counted		
Frequency of *Sordaria* occurrence relative to all samples		
Pre-LQE *Sordaria* average accumulation rates, range between parentheses (spores cm^{-2} yr^{-1}).		
Post-LQE *Sordaria* average accumulation rates, range between parentheses (spores cm^{-2} yr^{-1}).		
Total dung spores spores counted		
Frequency of dung spores occurrence relative to all samples		
Pre-LQE dung spores average accumulation rates, range between parentheses (spores cm^{-2} yr^{-1}).		
Post-LQE dun spores average accumulation rates, range between parentheses (spores cm^{-2} yr^{-1}).		

Ruppert Lake	Woody Bottom Pond
17 - 0	9.5 - 0
20	39
12 out of 48	17 out of 45
4.1 (0 - 39.0)	n/a
3.4 (0 -25.7)	8.4 (0 - 84.3)
36	47
17 out of 48	15 out of 45
2.6 (0 – 35.5)	n/a
6.7 (0 -46.0)	9.2 (0 – 77.8)
57	86
25 out of 48	22 out of 45
6.6 (0 - 39.0)	n/a
13.1 (0 - 56.5)	8.4 (0 - 84.3)

Suppl Tab 1

Supplementary Table 1: Samples used for pollen and spore analysis, *Lycopodium* batch numbers, age and accumulation rates from models plotted in Supplementary Figure 1.

* indicates ‘value extrapolated for plotting purposes’

Site	Date cored	Depth (cm)	sample	Lycopodium spores per tablet	Lycopodium batch number	Pollen	Spore	median sample age (ka)	sediment accumulation rate (cm/yr)
Ruppert Lake	2013	0	Ruppert Lake_0	12489	Batch 212761	Yes	Yes	-63	
Ruppert Lake	2013	27	Ruppert_27	12489	Batch 212761	Yes	Yes	584	0.04049
Ruppert Lake	2013	35	Ruppert_35	12489	Batch 212761	Yes	Yes	787.3	0.04065
Ruppert Lake	2013	59	Ruppert_59	12489	Batch 212761	Yes	Yes	1339.3	0.03968
Ruppert Lake	2013	67	Ruppert_67	12489	Batch 212761	No	Yes	1509	0.04926
Ruppert Lake	2013	83	Ruppert_83	12489	Batch 212761	Yes	Yes	1848.8	0.04237
Ruppert Lake	2013	91	Ruppert_91	12489	Batch 212761	Yes	Yes	2026.7	0.05587
Ruppert Lake	2013	99	Ruppert_99	12489	Batch 212761	Yes	Yes	2196	0.04464
Ruppert Lake	2013	123	Ruppert_123	12489	Batch 212761	Yes	Yes	3182.6	0.02203
Ruppert Lake	2013	139	Ruppert_139	12489	Batch 212761	Yes	Yes	4433.1	0.01003
Ruppert Lake	2013	155	Ruppert_155	12489	Batch 212761	Yes	Yes	5949.8	0.02000
Ruppert Lake	2013	163	Ruppert_163	12489	Batch 212761	Yes	Yes	6388.1	0.01828
Ruppert Lake	2013	171	Ruppert_171	12489	Batch 212761	Yes	Yes	6872.2	0.02101
Ruppert Lake	2013	179	Ruppert_179	12489	Batch 212761	Yes	Yes	7258.5	0.01757
Ruppert Lake	2013	187	Ruppert_187	12489	Batch 212761	Yes	Yes	7522.1	0.02370
Ruppert Lake	2013	203	Ruppert_203	12489	Batch 212761	Yes	Yes	8150.8	0.02353
Ruppert Lake	2013	230	Ruppert_230	12489	Batch 212761	Yes	Yes	9318.9	0.02451
Ruppert Lake	2013	245	Ruppert_245	12489	Batch 212761	Yes	Yes	9866.7	0.02421
Ruppert Lake	2013	247	Ruppert_247	12489	Batch 212761	Yes	Yes	10025.4	0.01294

Ruppert Lake	2013	251	Ruppert_251	12489	Batch 212761	Yes	Yes	10302.7	0.01263
Ruppert Lake	2013	263	Ruppert_263	12489	Batch 212761	Yes	Yes	11198.6	0.01277
Ruppert Lake	2013	280	Ruppert_280	12489	Batch 212761	Yes	Yes	12371.1	0.01553
Ruppert Lake	2013	283	Ruppert_283	12489	Batch 212761	No	Yes	12529.2	0.01969
Ruppert Lake	2013	299	Ruppert_299	12489	Batch 212761	No	Yes	13226.2	0.02110
Ruppert Lake	2013	315	Ruppert_315	12489	Batch 212761	Yes	Yes	13903.6	0.02257
Ruppert Lake	2013	331	Ruppert_331	12489	Batch 212761	Yes	Yes	14595.1	0.02217
Ruppert Lake	2013	335	Ruppert_335	12489	Batch 212761	Yes	Yes	14776	0.02315
Ruppert Lake	2013	347	Ruppert_347	12489	Batch 212761	Yes	Yes	15298.2	0.02257
Ruppert Lake	2013	351	Ruppert_351	12489	Batch 212761	Yes	Yes	15475	0.02288
Ruppert Lake	2013	365	Ruppert_365	12489	Batch 212761	No	Yes	16084.6	0.02387
Ruppert Lake	2013	367	Ruppert_367	12489	Batch 212761	Yes	Yes	16166.7	0.02488
Ruppert Lake	2013	371	Ruppert_371	12489	Batch 212761	No	Yes	16325.9	0.02558
Ruppert Lake	2013	372	Ruppert_372	12489	Batch 212761	No	Yes	16362.7	0.02717
Ruppert Lake	2013	373	Ruppert_373	12489	Batch 212761	No	Yes	16398.1	0.02825
Ruppert Lake	2013	374	Ruppert_374	12489	Batch 212761	No	Yes	16436.9	0.02577
Ruppert Lake	2013	375	Ruppert_375	12489	Batch 212761	No	Yes	16471	0.02933
Ruppert Lake	2013	376	Ruppert_376	12489	Batch 212761	No	Yes	16507.6	0.02732
Ruppert Lake	2013	377	Ruppert_377	12489	Batch 212761	No	Yes	16544.1	0.02740
Ruppert Lake	2013	378	Ruppert_378	12489	Batch 212761	No	Yes	16584.6	0.02469
Ruppert Lake	2013	379	Ruppert_379	12489	Batch 212761	No	Yes	16621.6	0.02703
Ruppert Lake	2013	380	Ruppert_380	12489	Batch 212761	No	Yes	16659.6	0.02632
Ruppert Lake	2013	381	Ruppert_381	12489	Batch 212761	No	Yes	16690.9	0.03195
Ruppert Lake	2013	382	Ruppert_382	12489	Batch 212761	No	Yes	16725.8	0.02865
Ruppert Lake	2013	383	Ruppert_383	12489	Batch 212761	No	Yes	16759.5	0.02967
Ruppert Lake	2013	384	Ruppert_384	12489	Batch 212761	No	Yes	16798.8	0.02545
Ruppert Lake	2013	385	Ruppert_385	12489	Batch 212761	No	Yes	16838.1 *	0.025445 *
Ruppert Lake	2013	386	Ruppert_386	12489	Batch 212761	No	Yes	16877.4 *	0.025445 *
Ruppert Lake	2013	387	Ruppert_387	12489	Batch 212761	No	Yes	16916.7 *	0.025445 *

Woody Bottom Pond	2013	0	WBP_0	12489	Batch 212761	Yes	Yes	-63	
Woody Bottom Pond	2013	4	WBP_4	12489	Batch 212761	Yes	Yes	110.2	0.02309
Woody Bottom Pond	2013	8	WBP_8	12489	Batch 212761	Yes	Yes	289.1	0.01969
Woody Bottom Pond	2013	12	WBP_12	12489	Batch 212761	Yes	Yes	480.2	0.02045
Woody Bottom Pond	2013	16	WBP_16	12489	Batch 212761	Yes	Yes	706.1	0.01445
Woody Bottom Pond	2013	40	WBP_40	12489	Batch 212761	Yes	Yes	2035.2	0.01761
Woody Bottom Pond	2013	44	WBP_44	12489	Batch 212761	Yes	Yes	2275.8	0.01757
Woody Bottom Pond	2013	48	WBP_48	12489	Batch 212761	Yes	Yes	2554.2	0.01183
Woody Bottom Pond	2013	52	WBP_52	12489	Batch 212761	Yes	Yes	2813.4	0.02151
Woody Bottom Pond	2013	56	WBP_56	12489	Batch 212761	Yes	Yes	3037.8	0.01488
Woody Bottom Pond	2013	60	WBP_60	12489	Batch 212761	Yes	Yes	3300	0.01715
Woody Bottom Pond	2013	64	WBP_64	12489	Batch 212761	Yes	Yes	3536.1	0.01718
Woody Bottom Pond	2013	68	WBP_68	12489	Batch 212761	Yes	Yes	3666.5	0.04630
Woody Bottom Pond	2013	72	WBP_72	12489	Batch 212761	Yes	Yes	3771.4	0.03135
Woody Bottom Pond	2013	76	WBP_76	12489	Batch 212761	Yes	Yes	3874.6	0.03846
Woody Bottom Pond	2013	80	WBP_80	12489	Batch 212761	Yes	Yes	3977.3	0.04525

Woody Bottom Pond	2013	84	WBP_84	12489	Batch 212761	Yes	Yes	4100	0.03165
Woody Bottom Pond	2013	88	WBP_88	12489	Batch 212761	Yes	Yes	4209.6	0.03521
Woody Bottom Pond	2013	96	WBP_96	12489	Batch 212761	Yes	Yes	4431.5	0.03663
Woody Bottom Pond	2013	100	WBP_100	12489	Batch 212761	Yes	Yes	4544.1	0.03559
Woody Bottom Pond	2013	104	WBP_104	12489	Batch 212761	Yes	Yes	4645.8	0.03378
Woody Bottom Pond	2013	108	WBP_108	12489	Batch 212761	Yes	Yes	4755.8	0.03401
Woody Bottom Pond	2013	112	WBP_112	12489	Batch 212761	Yes	Yes	4891.7	0.02364
Woody Bottom Pond	2013	116	WBP_116	12489	Batch 212761	Yes	Yes	5036.5	0.02457
Woody Bottom Pond	2013	120	WBP_120	12489	Batch 212761	Yes	Yes	5193.8	0.02874
Woody Bottom Pond	2013	124	WBP_124	12489	Batch 212761	Yes	Yes	5347.2	0.02653
Woody Bottom Pond	2013	128	WBP_128	12489	Batch 212761	Yes	Yes	5509.3	0.02242
Woody Bottom Pond	2013	132	WBP_132	12489	Batch 212761	Yes	Yes	5654.6	0.03472
Woody Bottom Pond	2013	136	WBP_136	12489	Batch 212761	Yes	Yes	5784	0.03106
Woody Bottom Pond	2013	140	WBP_140	12489	Batch 212761	Yes	Yes	5935.8	0.02237
Woody Bottom Pond	2013	144	WBP_144	12489	Batch 212761	Yes	Yes	6131.9	0.02183
Woody Bottom Pond	2013	148	WBP_148	12489	Batch 212761	Yes	Yes	6325.9	0.01988

Woody Bottom Pond	2013	152	WBP_152	12489	Batch 212761	Yes	Yes	6527.3	0.01838
Woody Bottom Pond	2013	156	WBP_156	12489	Batch 212761	Yes	Yes	6720.2	0.02101
Woody Bottom Pond	2013	160	WBP_160	12489	Batch 212761	Yes	Yes	6905.6	0.02392
Woody Bottom Pond	2013	164	WBP_164	12489	Batch 212761	No	Yes	7100.5	0.02016
Woody Bottom Pond	2013	168	WBP_168	12489	Batch 212761	Yes	Yes	7303.7	0.01727
Woody Bottom Pond	2013	172	WBP_172	12489	Batch 212761	Yes	Yes	7527.4	0.01859
Woody Bottom Pond	2013	176	WBP_176	12489	Batch 212761	Yes	Yes	7799.9	0.01005
Woody Bottom Pond	2013	180	WBP_180	12489	Batch 212761	Yes	Yes	8182.3	0.01074
Woody Bottom Pond	2013	184	WBP_184	12489	Batch 212761	Yes	Yes	8596.2	0.00934
Woody Bottom Pond	2013	188	WBP_188	12489	Batch 212761	Yes	Yes	8914.1	0.01242
Woody Bottom Pond	2013	192	WBP_192	12489	Batch 212761	Yes	Yes	9176.3	0.01842
Woody Bottom Pond	2013	196	WBP_196	12489	Batch 212761	No	Yes	9386	0.01848
Woody Bottom Pond	2013	200	WBP_200	12489	Batch 212761	Yes	Yes	9595.7 *	0.01848 *
Jan Lake	1994	151	Jan_151	13911	Batch 710961	Yes	Yes	4649.1	0.03289
Jan Lake	1994	161	Jan_161	12077	Unknown at the time of writing	Yes	Yes	5119.2	0.01704
Jan Lake	1994	181	Jan_181	12077	Unknown at the time of writing	Yes	Yes	6195.5	0.02160
Jan Lake	1994	191	Jan_191	13911	Batch 710961	Yes	Yes	6656	0.02141

Jan Lake	1994	201	Jan_201	12077	Unknown at the time of writing	Yes	Yes	7120.5	0.02564
Jan Lake	1994	213	Jan_213	13911	Batch 710961	Yes	Yes	7874.5	0.01166
Jan Lake	1994	221	Jan_221	12077	Unknown at the time of writing	Yes	Yes	8704.6	0.00818
Jan Lake	1994	232	Jan_232	12077	Unknown at the time of writing	Yes	Yes	9958.6	0.03448
Jan Lake	1994	250	Jan_250	12077	Unknown at the time of writing	Yes	Yes	10485.4	0.03559
Jan Lake	1994	270	Jan_270	13911	Batch 710961	Yes	Yes	11094.7	0.03448
Jan Lake	1994	280	Jan_280	13911	Batch 710961	Yes	Yes	11398.5	0.04167
Jan Lake	1994	291	Jan_291	13911	Batch 710961	Yes	Yes	11638.7	0.04444
Jan Lake	1994	296	Jan_296	13911	Batch 710961	Yes	Yes	11757.9	0.04049
Jan Lake	1994	301	Jan_301	13911	Batch 710961	Yes	Yes	11877.3	0.03891
Jan Lake	1994	307	Jan_307	13911	Batch 710961	Yes	Yes	12071.4	0.02639
Jan Lake	1994	311	Jan_311	13911	Batch 710961	Yes	Yes	12220.7	0.02008
Jan Lake	1994	321	Jan_321	13911	Batch 710961	Yes	Yes	12720.1	0.01862
Jan Lake	1994	331	Jan_331	13911	Batch 710961	Yes	Yes	13263.3	0.01946
Jan Lake	1994	338	Jan_338	13911	Batch 710961	Yes	Yes	13638.8	0.01883
Jan Lake	1994	348	Jan_348	13911	Batch 710961	Yes	Yes	14150.4	0.02155
Windmill Lake	1994	730	Windmill_730	12542	Batch 124961	Yes	Yes	9466	0.02128
Windmill Lake	1994	740	Windmill_740	11267	Batch 201890	Yes	Yes	9940	0.02174
Windmill Lake	1994	755	Windmill_755	13911	Batch 710961	Yes	Yes	10588	0.02273
Windmill Lake	1994	770	Windmill_770	13911	Batch 710961	Yes	Yes	11217	0.02439
Windmill Lake	1994	795	Windmill_795	13911	Batch 710961	Yes	Yes	12537	0.01471
Windmill Lake	1994	802	Windmill_802	12542	Batch 124961	Yes	Yes	12999	0.01587
Windmill Lake	1994	815	Windmill_815	13911	Batch 710961	Yes	Yes	13702	0.02381
Windmill Lake	1994	823	Windmill_823	13911	Batch 710961	Yes	Yes	14010	0.02564
Windmill Lake	1994	830	Windmill_830	13911	Batch 710961	Yes	Yes	14248	0.03226
Windmill Lake	1994	845	Windmill_845	13911	Batch 710961	Yes	Yes	14548	0.05000

Windmill Lake	1994	855	Windmill_855	13911	Batch 710961	Yes	Yes	14755	0.05000

Supplementary Table 2: Bone samples plotted on Figure 1 and Figure 2

Taxon	LatDD	LongDD	Lab number	14C date	error	Cal. from	Cal. to	Cal. median	AMS date
Alces	69.34	-154.68	Beta-339275	116	0.3	260	29	104	√
Alces	69.53	-156.29	Beta-339266	107	0.3	255	31	122	√
Alces	69.50	-154.40	Beta-339280	210	30	305	…	179	√
Alces	69.68	-156.86	Beta-339271	290	30	458	288	384	√
Alces	69.34	-154.68	Beta-339281	310	30	465	301	387	√
Alces	70.70	-154.53	CAMS-91966	320	35	474	304	388	√
Alces	69.33	-138.00	RIDDL-544	550	120	704	315	563	√
Alces	70.70	-154.53	CAMS-92094	665	35	678	556	629	√
Alces	70.70	-154.53	Beta-339274	950	30	926	795	854	√
Alces	70.70	-154.53	CAMS-64459	980	40	959	795	872	√
Alces	67.80	-139.92	Beta-33190	985	70	1053	740	885	√
Alces	64.93	-147.64	AA-14253	1158	52	1232	959	1080	√
Alces	70.70	-154.53	Beta-339268	1180	30	1221	999	1112	√
Alces	64.93	-147.64	AA-14252	1200	62	1269	981	1127	√
Alces	70.70	-154.53	Beta-134225	1280	40	1294	1086	1225	√
Alces	70.70	-154.53	CAMS-64474	1370	40	1351	1186	1294	√
Alces	70.70	-154.53	CAMS-64467	1760	40	1810	1566	1668	√
Alces	69.01	-153.91	Beta-135071	2330	50	2679	2159	2350	√
Alces	70.70	-154.53	CAMS-92076	2450	35	2705	2360	2528	√
Alces	69.01	-153.91	CAMS-58096	2460	40	2710	2364	2552	√
Alces	70.70	-154.53	CAMS-64418	2540	50	2756	2464	2613	√
Alces	70.70	-154.53	Beta-339282	2790	30	2960	2795	2890	√
Alces	69.53	-156.29	Beta-263035	2900	40	3165	2925	3036	√
Alces	65.04	-147.11	AA-14329	3401	79	3845	3457	3656	√

Alces	64.93	-147.64	AA-14271	3539	58	3978	3647	3823	√
Alces	64.93	-147.64	AA-14285	3941	52	4526	4236	4382	√
Alces	64.81	-164.50	AA-14324	3983	65	4798	4238	4455	√
Alces	65.04	-147.11	AA-14279	3992	54	4784	4258	4470	√
Alces	63.98	-140.78	TO-2356	4040	60	4815	4408	4530	√
Alces	65.04	-147.11	AA-14292	4164	56	4839	4530	4698	√
Alces	69.00	-132.00	RIDDL-545	4360	100	5306	4651	4976	√
Alces	65.00	-147.00	AA-14267	4414	54	5281	4859	5011	√
Alces	65.04	-147.11	AA-14262	4447	53	5288	4877	5084	√
Alces	65.50	-150.17	AA-14236	5294	61	6264	5930	6080	√
Alces	65.98	-147.32	DIC-2416	5380	55	6287	6003	6182	
Alces	65.04	-147.11	AA-14254	5534	59	6445	6211	6338	√
Alces	64.93	-147.64	AA-14286	5805	56	6740	6476	6604	√
Alces	64.84	-147.96	AA-14282	5941	90	7004	6531	6777	√
Alces	64.93	-147.64	AA-14333	6022	54	7139	6730	6866	√
Alces	65.04	-147.11	AA-14243	6221	138	7420	6797	7111	√
Alces	65.04	-147.11	AA-14255	6361	62	7420	7174	7299	√
Alces	65.04	-147.11	AA-14240	6396	62	7430	7178	7331	√
Alces	65.04	-147.11	AA-14264	6621	60	7586	7428	7510	√
Alces	65.04	-147.11	AA-14241	6631	69	7614	7425	7517	√
Alces	65.04	-147.11	AA-14283	6667	59	7650	7434	7537	√
Alces	65.04	-147.11	AA-14331	6676	92	7685	7424	7547	√
Alces	64.81	-164.50	AA-14303	6711	69	7680	7460	7578	√
Alces	65.04	-147.11	AA-14265	6716	61	7675	7479	7583	√
Alces	65.04	-147.11	AA-14284	6727	58	7677	7493	7593	√
Alces	65.04	-147.11	AA-14332	6761	76	7755	7480	7618	√
Alces	65.04	-147.11	AA-14339	6774	70	7758	7505	7627	√
Alces	65.04	-147.11	AA-14325	6788	60	7746	7517	7635	√
Alces	64.81	-164.50	AA-14328	6791	65	7784	7515	7637	√
Alces	65.04	-147.11	AA-14342	6998	71	7952	7688	7830	√
Alces	64.96	-147.62	AA-14246	7121	94	8164	7755	7945	√
Alces	65.04	-147.11	AA-14341	7128	104	8172	7739	7952	√
Alces	64.93	-147.64	AA-14336	7484	53	8387	8191	8302	√
Alces	65.00	-148.00	DIC-2414	8740	70	10125	9543	9738	
Alces	65.04	-147.11	AA-14245	8839	83	10190	9630	9918	√
Alces	65.04	-147.11	AA-14290	8856	79	10196	9678	9950	√
Alces	64.96	-147.62	AA-14248	8858	80	10198	9677	9953	√
Alces	65.00	-147.00	AA-14273	8877	77	10198	9702	9985	√
Alces	64.96	-147.62	AA-14340	9000	80	10373	9795	10138	√
Alces	65.04	-147.11	AA-14242	9114	81	10520	9974	10296	√
Alces	69.68	-156.86	Beta-339283	9310	40	10654	10303	10518	√
Alces	65.04	-147.11	AA-14259	9503	96	11162	10562	10831	√
Alces	64.93	-147.64	AA-14256	9589	91	11198	10684	10936	√

Alces	70.70	-154.53	Beta-339270	9610	40	11161	10775	10937	√
Alces	65.04	-147.11	AA-14270	9618	80	11196	10734	10954	√
Alces	65.04	-147.11	AA-14338	9650	77	11207	10757	10985	√
Alces	64.93	-147.64	AA-14257	9685	88	11239	10761	11040	√
Alces	64.84	-147.96	AA-14337	9717	65	11248	10792	11138	√
Alces	65.04	-147.11	AA-14249	9872	86	11701	11151	11314	√
Alces	64.81	-164.50	AA-14238	9927	67	11694	11213	11364	√
Alces	64.81	-164.50	AA-14276	10033	90	11956	11250	11559	√
Alces	65.00	-150.62	AA-14269	10053	76	11956	11272	11586	√
Alces	61.50	-148.80	AA-14277	10062	77	11968	11285	11606	√
Alces	65.00	-150.62	AA-14237	10069	111	12025	11255	11632	√
Alces	65.04	-147.11	AA-14247	10103	92	12044	11315	11691	√
Alces	65.04	-147.11	AA-14326	10756	64	12749	12577	12687	√
Alces	65.00	-147.00	AA-14274	11000	80	13040	12725	12874	√
Alces	66.23	-161.25	AA-14263	11127	79	13129	12789	12983	√
Alces	65.12	-147.53	AA-14250	11210	81	13256	12860	13076	√
Alces	64.84	-147.64	AA-14258	11267	95	13321	12912	13134	√
Alces	67.10	-140.50	CAMS-23472	11570	60	13543	13279	13400	√
Alces	65.04	-147.11	AA-14334	11671	76	13714	13331	13502	√
Alces	65.12	-147.53	AA-14291	11678	81	13720	13344	13508	√
Alces	65.04	-147.11	AA-14244	11790	117	13945	13390	13623	√
Alces	65.04	-147.11	AA-14327	11947	89	14030	13565	13790	√
Alces	64.40	-141.23	AA-14268	11988	82	14062	13601	13848	√
Alces	65.04	-147.11	AA-14260	12022	153	14335	13473	13893	√
Alces	65.04	-147.11	AA-14266	12201	85	14475	13780	14098	√
Alces	70.70	-154.53	CAMS-91810	12245	40	14314	14000	14143	√
Bison	61.20	-149.90	Beta 136732	170	30	291	...	178	√
Bison	67.64	-144.58	Beta 62999	1730	60	1815	1532	1646	√
Bison	67.64	-144.58	OxA-11248	2172	37	2313	2061	2203	√
Bison	66.26	-145.82	OxA-11990	2415	25	2680	2353	2430	√
Bison	61.57	-135.83	Beta 137731	2460	40	2710	2364	2552	√
Bison	66.26	-145.82	OxA-11989	2526	26	2743	2495	2616	√
Bison	67.64	-144.58	OxA-11631	2776	36	2955	2785	2872	√
Bison	66.66	-143.72	Beta 136731	4390	70	5284	4842	4992	√
Bison	67.64	-144.58	Beta 65662	4495	60	5316	4892	5149	√
Bison	67.57	-136.42	Beta-18552	9000	250	10779	9498	10113	√
Bison	64.21	-145.04	OxA-11246	9400	55	10765	10441	10630	√
Bison	69.36	-139.53	RIDDL-319	9400	230	11306	9961	10683	√
Bison	64.21	-145.04	OxA-11962	9506	38	11073	10660	10784	√
Bison	62.64	-141.00	Beta 241522	9580	60	11152	10724	10934	√
Bison	69.36	-139.53	RIDDL-281	9770	180	11819	10592	11181	√
Bison	69.36	-139.53	RIDDL-362	9870	180	11995	10759	11374	√

Bison	70.70	-154.53	CAMS 53767	10510	50	12644	12173	12475	√
Bison	69.50	-154.40	CAMS-53767	10510	50	12644	12173	12475	√
Bison	70.70	-154.53	CAMS 53891	10990	50	12996	12729	12849	√
Bison	69.70	-153.80	CAMS-53891	10990	50	12996	12729	12849	√
Bison	67.57	-139.83	QU-780	11450	400	14508	12565	13352	
Bison	70.70	-154.53	CAMS-53756	11810	50	13756	13485	13643	√
Bison	67.44	-133.75	OxA-18549	11830	45	13758	13554	13655	√
Bison	67.64	-144.58	Beta 67494	11900	70	13954	13556	13711	√
Bison	66.26	-145.82	Beta-67494	11900	70	13954	13556	13711	√
Bison	67.64	-144.58	RS-9200	11900	70	13954	13556	13711	
Bison	65.40	-147.10	ST-11633	11980	135	14160	13487	13840	
Bison	62.64	-141.00	Beta 241523	12020	70	14078	13731	13879	√
Bison	70.70	-154.53	CAMS 53774	12270	50	14487	14011	14185	√
Bison	69.50	-154.40	CAMS-53774	12270	50	14487	14011	14185	√
Bison	69.50	-154.40	CAMS-58091	12320	60	14686	14070	14299	√
Bison	64.07	-141.89	OxA-10679	12340	65	14742	14081	14355	√
Bison	67.57	-139.83	OxA-10546	12350	70	14784	14082	14384	√
Bison	64.07	-141.89	OxA-11226	12380	60	14805	14123	14434	√
Bison	70.70	-154.53	CAMS 53760	12410	50	14846	14168	14492	√
Bison	69.70	-153.80	CAMS-53760	12410	50	14846	14168	14492	√
Bison	67.64	-144.58	OxA-12067	12425	45	14875	14197	14524	√
Bison	64.07	-141.89	OxA-111	12465	75	15045	14220	14625	√
Bison	64.07	-141.89	OXA-10541	12525	70	15115	14320	14785	√
Bison	69.50	-154.40	AA-48281	12560	130	15247	14218	14804	√
Bison	67.57	-139.83	QU-783	12220	1500	19488	10877	14896	
Bison	67.57	-139.83	TO-34	12610	70	15241	14576	14963	√
Bison	67.57	-139.83	QU-782	12660	560	16681	13470	15010	
Bison	64.07	-141.89	OxA-10855	12655	65	15268	14743	15050	√
Bison	65.40	-147.10	AA26829	12860	140	15840	14894	15368	√
Bison	64.07	-141.89	OxA-10544	12915	70	15703	15198	15433	√
Bison	64.04	-139.42	OxA-11197	12960	60	15735	15266	15492	√
Bison	64.07	-141.89	OxA-10538	12960	70	15754	15249	15494	√
Bison	69.33	-138.00	K-1327	13010	350	16582	14246	15545	
Bison	66.66	-138.63	OxA-10681	13040	70	15868	15318	15616	√
Bison	65.30	-148.40	OxA-11277	13125	75	16025	15437	15755	√
Bison	66.66	-138.63	OxA-11166	13135	65	16028	15503	15774	√
Bison	64.07	-141.89	OxA-10540	13160	70	16067	15553	15810	√

Bison	65.04	-147.11	OxA-11617	13235	65	16128	15694	15910	√
Bison	64.07	-141.89	OxA-10543	13240	75	16162	15680	15916	√
Bison	66.46	-161.37	OxA-11223	16685	80	20389	19895	20133	√
Bison	70.70	-154.53	CAMS-53777	17160	80	20946	20476	20698	√
Bison	64.07	-141.89	OxA-10542	17960	90	22019	21469	21756	√
Bison	70.70	-154.53	CAMS 53772	19420	100	23682	23046	23386	√
Bison	69.50	-154.40	CAMS-53772	19420	100	23682	23046	23386	√
Bison	60.26	-149.45	OxA-11247	19420	100	23682	23046	23386	√
Bison	64.07	-141.89	OxA-11139	19540	120	23893	23146	23544	√
Bison	69.50	-154.40	CAMS-53890	21040	120	25679	25093	25394	√
Cervus	65.04	-147.11	AA-25963	262	44	463	...	315	√
Cervus	69.36	-139.53	TO-5681	3010	60	3361	3006	3197	√
Cervus	64.07	-141.89	AA-14317	4462	52	5298	4886	5120	√
Cervus	64.07	-141.89	AA-14313	5641	63	6601	6297	6425	√
Cervus	64.92	-147.60	AA-25960	8650	90	10111	9477	9648	√
Cervus	64.07	-141.89	AA-14315	9793	99	11604	10788	11212	√
Cervus	64.07	-141.89	AA-26023	10120	110	12107	11275	11725	√
Cervus	65.04	-147.11	AA-14287	10159	78	12096	11404	11816	√
Cervus	64.84	-147.96	AA-25975	10292	111	12529	11625	12085	√
Cervus	64.84	-147.96	AA-25956	10330	120	12564	11708	12158	√
Cervus	64.00	-142.00	AA-14304	10533	83	12687	12145	12480	√
Cervus	64.70	-145.00	AA-14304	10533	83	12687	12145	12480	√
Cervus	64.00	-142.00	AA-14301	10805	84	12859	12565	12715	√
Cervus	67.13	-140.78	CAMS-23467	10820	60	12810	12651	12721	√
Cervus	63.97	-138.97	OxA-20920	10825	50	12795	12675	12722	√
Cervus	64.84	-147.96	AA-14295	11644	79	13705	13292	13473	√
Cervus	65.04	-147.11	AA-14302	11664	96	13720	13308	13496	√
Cervus	65.00	-141.00	OxA-20918	11675	45	13581	13425	13506	√
Cervus	65.00	-141.00	OxA-20919	11785	50	13737	13479	13619	√
Cervus	65.04	-147.11	AA-25964	11837	83	13822	13461	13655	√
Cervus	65.12	-147.53	AA-25964	11837	83	13822	13461	13655	√
Cervus	64.93	-147.64	AA-25974	11984	131	14161	13495	13844	√
Cervus	64.92	-147.60	AA-25990	11980	152	14214	13466	13844	√
Cervus	64.84	-147.96	AA-25977	12021	132	14218	13554	13886	√
Cervus	65.12	-147.53	AA-25966	12026	136	14256	13549	13892	√
Cervus	64.92	-147.60	AA-14293	12096	81	14151	13756	13950	√
Cervus	65.04	-147.11	AA-25987	12110	133	14499	13588	13988	√
Cervus	65.12	-147.53	AA-14307	12170	93	14405	13758	14052	√
Cervus	64.81	-164.50	AA-14316	12172	82	14318	13766	14053	√
Cervus	65.04	-147.11	AA-25970	12160	130	14666	13735	14059	√
Cervus	65.04	-147.11	AA-25969	12185	139	14752	13739	14111	√

Cervus	64.84	-147.96	AA-25976	12201	135	14752	13750	14138	√
Cervus	64.92	-147.60	AA-25985	12212	136	14777	13753	14161	√
Cervus	64.92	-147.60	AA-25994	12237	208	15094	13719	14280	√
Cervus	65.12	-147.53	AA-14306	12281	114	14846	13848	14289	√
Cervus	64.93	-147.64	AA-25971	12270	140	14906	13791	14291	√
Cervus	65.04	-147.11	AA-25978	12276	135	14907	13810	14300	√
Cervus	65.12	-147.53	AA-25989	12282	136	14925	13819	14314	√
Cervus	65.12	-147.53	AA-25993	12281	148	14953	13800	14323	√
Cervus	65.12	-147.53	AA-14319	12346	84	14847	14058	14393	√
Cervus	65.12	-147.53	AA-25992	12321	138	15037	13931	14394	√
Cervus	64.92	-147.60	AA-14296	12359	83	14871	14076	14417	√
Cervus	64.92	-147.60	AA-14303	12355	93	14908	14060	14420	√
Cervus	64.92	-147.60	AA-25958	12340	130	15025	13984	14423	√
Cervus	64.07	-141.89	AA-25959	12350	140	15063	13981	14446	√
Cervus	64.83	-148.00	AA-25981	12377	135	15068	14033	14488	√
Cervus	64.92	-147.60	AA-25982	12413	149	15124	14049	14550	√
Cervus	64.92	-147.60	AA-25961	12425	130	15094	14100	14563	√
Cervus	65.12	-147.53	AA-14300	12443	102	15059	14156	14584	√
Cervus	66.95	-150.93	AA-14314	12437	139	15121	14096	14584	√
Cervus	64.84	-147.96	AA-25979	12438	137	15118	14100	14585	√
Cervus	64.96	-147.62	AA-14309	12446	94	15046	14170	14588	√
Cervus	64.84	-147.96	AA-25986	12441	150	15146	14076	14593	√
Cervus	64.92	-147.60	AA-25983	12455	139	15135	14110	14613	√
Cervus	64.92	-147.60	AA-14298	12468	94	15076	14196	14632	√
Cervus	64.92	-147.60	AA-25980	12473	144	15162	14115	14643	√
Cervus	65.04	-147.11	AA-14318	12473	84	15069	14219	14644	√
Cervus	64.96	-147.62	AA-25988	12480	139	15158	14130	14654	√
Cervus	65.12	-147.53	AA-14299	12500	106	15127	14209	14698	√
Cervus	65.74	-149.10	AA-14311	12501	105	15127	14212	14701	√
Cervus	66.95	-150.93	AA-14321	12518	85	15121	14275	14752	√
Cervus	65.04	-147.11	AA-14322	12549	88	15161	14302	14820	√
Cervus	64.92	-147.60	AA-14297	12562	94	15190	14305	14840	√
Cervus	65.12	-147.53	AA-14308	12584	95	15229	14341	14883	√
Cervus	65.12	-147.53	AA-14294	12577	83	15209	14382	14884	√
Cervus	65.12	-147.53	AA-25962	12620	130	15341	14260	14919	√
Cervus	64.92	-147.60	AA-25957	12640	140	15433	14256	14952	√
Cervus	64.92	-147.60	AA-14323	12657	89	15338	14577	15032	√
Cervus	64.92	-147.60	AA-25955	12770	240	15921	14221	15172	√
Equus	70.57	-153.64	Beta-339279	10570	40	12660	12422	12558	√
Equus	69.52	-153.09	Beta-331878	11710	50	13712	13432	13524	√
Equus	63.30	-146.03	AA-74249	11950	100	14056	13560	13796	√
Equus	64.40	-147.30	CAMS-119982	12310	100	14865	13980	14338	√

Equus	64.40	-147.30	AA-37609	12380	120	15034	14062	14485	√
Equus	69.50	-154.40	CAMS-92091	12465	40	14970	14273	14628	√
Equus	69.50	-154.40	CAMS-120651[#]	12480	35	14997	14309	14681	√
Equus	69.50	-154.40	CAMS-121738[#]	12490	45	15036	14314	14708	√
Equus	64.40	-147.30	AA26819	12510	130	15176	14170	14710	√
Equus	64.40	-147.30	CAMS-145101	12510	45	15081	14377	14772	√
Equus	64.50	-147.60	AA26810	12560	140	15265	14195	14798	√
Equus	64.40	-147.30	CAMS-145091	12560	45	15139	14569	14894	√
Equus	64.40	-147.30	CAMS-145092	12670	60	15275	14784	15080	√
Equus	69.50	-154.40	CAMS-120673	12780	35	15364	15089	15223	√
Equus	64.40	-147.30	AA-37614	12840	140	15805	14829	15336	√
Equus	65.40	-147.10	AA26829	12860	140	15840	14894	15368	√
Equus	67.10	-140.50	GSC-2881	12900	100	15748	15129	15421	
Equus	69.50	-154.40	Beta-331866	12980	50	15740	15298	15520	√
Equus	69.54	-156.06	Beta-331882	13010	60	15796	15308	15569	√
Equus	64.40	-147.30	CAMS-145095	13055	50	15857	15369	15646	√
Equus	64.40	-148.00	AA26811	13270	150	16375	15436	15948	√
Equus	69.54	-156.06	Beta-331883	13400	50	16299	15924	16125	√
Equus	69.50	-154.40	CAMS-91792	13685	40	16747	16300	16503	√
Equus	69.50	-154.40	CAMS-120655	13925	40	17071	16631	16886	√
Equus	64.40	-147.30	AA26805	14000	160	17480	16487	16994	√
Equus	64.50	-147.40	AA26817	14120	180	17662	16592	17167	√
Equus	64.40	-148.00	AA26840	14260	160	17833	16907	17357	√
Equus	69.54	-156.06	Beta-263037	14290	70	17620	17158	17408	√
Equus	65.00	-147.40	OxA-16361	14300	160	17868	16975	17410	√
Equus	69.54	-156.06	Beta-331887	14360	60	17703	17263	17502	√
Equus	69.54	-156.06	CAMS-120711	14540	45	17910	17550	17721	√
Equus	67.10	-140.50	OxA-17691	14715	55	18079	17710	17909	√
Equus	64.40	-147.30	AA26852	14990	190	18670	17808	18226	√
Equus	56.60	-133.30	Beta-109267	15090	70	18551	18107	18341	√
Equus	69.50	-154.40	CAMS-120676	15095	40	18505	18162	18350	√

Equus	64.40	-147.30	CAMS-119977	15460	100	18920	18517	18724	√
Equus	64.50	-147.30	AA26812	15570	190	19301	18421	18837	√
Equus	69.24	-154.03	Beta-258461	15630	70	19036	18723	18872	√
Equus	64.40	-147.30	AA26808	15750	190	19511	18651	19037	√
Equus	64.40	-147.30	CAMS-145109	15810	70	19270	18881	19062	√
Equus	65.80	-163.22	K-1210	15750	350	19938	18322	19073	
Equus	64.40	-147.30	CAMS-120068	15850	100	19421	18881	19117	√
Equus	64.40	-147.30	CAMS-145104	15920	70	19446	18977	19198	√
Equus	64.40	-147.30	AA26820	15920	190	19670	18794	19220	√
Equus	64.50	-147.60	AA26837	16130	240	20045	18910	19466	√
Equus	64.40	-147.30	AA26845	16150	210	20009	18972	19488	√
Equus	69.41	-153.47	Beta-331891	16170	60	19716	19290	19519	√
Equus	64.40	-147.30	CAMS-119968	16370	100	20034	19514	19762	√
Equus	65.58	-139.08	RIDDL-765/ RIDDL-766	16391	121	20094	19495	19784	√
Equus	65.00	-147.20	AA26807	16700	220	20681	19601	20158	√
Equus	69.50	-154.40	CAMS-120683	16885	45	20545	20166	20370	√
Equus	69.50	-154.40	CAMS-120685	16925	45	20586	20221	20417	√
Equus	69.50	-154.40	CAMS-92073	17290	60	21065	20640	20849	√
Equus	69.50	-154.40	CAMS-120700	17300	60	21080	20650	20861	√
Equus	67.10	-140.50	RIDDL-278	17440	220	21703	20523	21081	√
Equus	65.58	-139.08	Beta 185981	17490	90	21435	20838	21128	√
Equus	69.54	-156.06	Beta-283250	17670	70	21651	21080	21379	√
Equus	69.54	-155.19	Beta-331862	17720	70	21736	21171	21452	√
Equus	64.40	-147.30	CAMS-145098	17770	80	21810	21238	21524	√
Equus	64.40	-147.30	AA26839	18890	280	23525	22236	22800	√
Equus	65.40	-147.10	AA26821	18910	280	23540	22265	22820	√
Equus	64.40	-147.30	CAMS-120058	19000	100	23185	22544	22871	√
Equus	64.40	-147.30	AA26824	19120	290	23741	22431	23055	√
Equus	69.50	-154.40	I-9371	19250	360	24037	22440	23212	
Equus	64.50	-147.40	AA26801	19390	290	24048	22655	23359	√
Equus	64.40	-147.30	AA26836	19450	280	24105	22755	23429	√
Equus	64.40	-147.30	AA26823	19460	320	24195	22670	23443	√

Equus	65.40	-147.10	AA26816	19470	290	24151	22755	23453	√
Equus	65.30	-147.10	AA26827	19560	300	24282	22850	23560	√
Equus	64.40	-147.30	CAMS-120059	19590	100	23930	23285	23607	√
Equus	64.40	-147.30	CAMS-145097	19630	100	23961	23354	23653	√
Equus	64.40	-147.30	CAMS-145096	19720	100	24035	23463	23751	√
Equus	64.40	-147.30	CAMS-145103	19760	100	24073	23505	23792	√
Equus	64.40	-147.30	CAMS-145108	19780	100	24093	23525	23813	√
Equus	64.40	-147.30	AA26849	19790	335	24676	22961	23830	√
Equus	64.40	-147.30	AA-37611	19800	280	24495	23109	23836	√
Equus	64.40	-147.30	CAMS-145116	19810	100	24125	23554	23845	√
Equus	64.40	-147.30	CAMS-145093	19830	100	24148	23575	23868	√
Equus	65.90	-147.10	AA26834	19835	155	24265	23489	23872	√
Equus	64.50	-147.40	AA26863	19835	155	24265	23489	23872	√
Equus	65.40	-147.10	AA26841	19830	330	24742	23024	23877	√
Equus	69.50	-154.40	CAMS-120656 #	19880	70	24158	23679	23928	√
Equus	69.50	-154.40	CAMS-121741 #	19900	60	24170	23720	23952	√
Equus	64.40	-147.30	CAMS-119983	19950	100	24290	23715	24007	√
Equus	64.40	-147.30	CAMS-119980	19960	100	24300	23730	24018	√
Equus	64.00	-139.20	AAR-11188	19990	140	24399	23685	24051	√
Equus	69.50	-154.40	CAMS-91964	20050	70	24340	23890	24114	√
Equus	64.40	-147.30	CAMS-145105	20150	110	24500	23934	24218	√
Equus	69.54	-156.06	CAMS-120703	20190	70	24483	24030	24258	√
Equus	64.40	-147.30	CAMS-145102	20210	110	24565	23975	24280	√
Equus	64.50	-147.40	AA26813	20170	329	25210	23532	24299	√
Equus	65.40	-147.10	AA-37608	20200	310	25195	23603	24332	√
Equus	64.40	-147.30	CAMS-145106	20430	90	24958	24265	24558	√
Equus	64.40	-147.30	CAMS-119978	20440	100	24995	24261	24582	√
Equus	64.50	-147.30	AA26862	20410	320	25433	23850	24606	√
Equus	64.40	-147.30	AA26869	20420	325	25455	23855	24619	√
Equus	64.40	-147.30	AA26866	20545	345	25596	23966	24762	√
Equus	64.50	-147.30	AA26857	20580	160	25258	24339	24789	√

Equus	69.50	-154.40	CAMS-120647 [#]	20640	80	25189	24518	24862	√
Equus	62.50	-141.00	Beta-70102	20660	100	25235	24514	24888	√
Equus	64.50	-147.40	AA-37613	20670	350	25700	24089	24894	√
Equus	64.40	-147.30	CAMS-145113	20720	110	25311	24545	24975	√
Equus	69.50	-154.40	CAMS-121734 [#]	20720	90	25286	24575	24985	√
Equus	64.40	-147.30	CAMS-145107	20730	90	25297	24583	25000	√
Equus	69.50	-154.40	I-9274	20810	410	25899	24119	25042	
Equus	64.40	-147.30	AA26850	20840	350	25840	24275	25084	√
Equus	64.40	-147.30	CAMS-145110	20810	120	25460	24615	25104	√
Equus	69.50	-154.40	CAMS-91802	20850	80	25481	24872	25176	√
Mammuthus	65.26	-166.35	Beta-13811	11360	100	13415	13059	13211	√
Mammuthus	64.75	-156.84	AA-22573	11500	160	13709	13064	13341	√
Mammuthus	64.25	-145.83	AA-17601	11540	140	13706	13096	13374	√
Mammuthus	68.87	-166.20	AA-26006	11910	130	14062	13470	13747	√
Mammuthus	64.25	-145.83	CAMS-17045	12060	70	14095	13753	13910	√
Mammuthus	64.25	-145.83	AA-74251	12050	120	14205	13579	13912	√
Mammuthus	64.25	-145.83	AA-74250	12110	120	14440	13625	13980	√
Mammuthus	64.94	-147.79	AA-14940	12123	88	14212	13755	13984	√
Mammuthus	69.50	-154.40	AA-17614	12190	130	14707	13750	14112	√
Mammuthus	66.90	-162.59	AA-77015	12300	70	14690	14030	14270	√
Mammuthus	65.12	-147.53	AA-14938	12337	108	14942	14013	14401	√
Mammuthus	64.93	-147.64	AA-14860	12429	178	15210	13995	14580	√
Mammuthus	65.60	-168.08	AA-26017	12440	130	15105	14114	14587	√
Mammuthus	65.12	-147.53	AA-14916	12476	81	15069	14227	14651	√
Mammuthus	69.50	-154.40	AA-14954	12490	170	15250	14080	14671	√
Mammuthus	66.23	-161.25	AA-14357	12508	145	15205	14143	14703	√
Mammuthus	64.94	-147.79	AA-14880	12576	147	15305	14185	14824	√
Mammuthus	68.10	-151.80	Beta-226405 & CAMS-131222	12585	75	15210	14447	14910	√
Mammuthus	65.10	-151.00	AA-14888	12677	142	15555	14330	15028	√
Mammuthus	64.94	-147.79	AA-14909	12884	124	15816	15043	15403	√
Mammuthus	63.57	-156.01	Beta-9906	12980	250	16311	14640	15523	√
Mammuthus	64.94	-147.79	AA-14947	13060	150	16083	15206	15641	√
Mammuthus	66.65	-147.50	AA-14925	13226	85	16175	15629	15898	√
Mammuthus	66.65	-147.50	AA-14925	13226	85	16175	15629	15898	√
Mammuthus	67.13	-140.78	CRNL-1220c	13280	390	17222	14727	15963	√
Mammuthus	68.35	-166.76	AA-26028	13290	140	16400	15534	15977	√
Mammuthus	68.35	-166.76	AA-26028	13290	140	16400	15534	15977	√

Mammuthus	64.94	-147.79	AA-14867	13339	150	16515	15602	16043	√
Mammuthus	64.94	-147.79	AA-14867	13339	150	16515	15602	16043	√
Mammuthus	64.88	-146.86	AA-14944	13380	88	16354	15810	16098	√
Mammuthus	67.13	-140.78	RIDDL-279	13390	180	16691	15579	16115	√
Mammuthus	64.85	-148.04	AA-14883	13410	152	16616	15708	16140	√
Mammuthus	65.12	-147.53	AA-14934	13436	87	16463	15889	16168	√
Mammuthus	65.12	-147.53	AA-14934	13436	87	16463	15889	16168	√
Mammuthus	65.26	-166.35	Beta-35841	13570	120	16781	16009	16361	√
Mammuthus	65.26	-166.35	Beta-35841	13570	120	16781	16009	16361	√
Mammuthus	64.40	-141.23	AA-14889	13661	156	16997	16059	16498	√
Mammuthus	64.40	-141.23	AA-14889	13661	156	16997	16059	16498	√
Mammuthus	64.74	-155.49	AA-25999	13690	190	17129	16008	16548	√
Mammuthus	64.74	-155.49	AA-25999	13690	190	17129	16008	16548	√
Mammuthus	66.90	-142.50	Beta-29166	13725	110	16960	16244	16581	√
Mammuthus	66.90	-142.50	Beta-29166	13725	110	16960	16244	16581	√
Mammuthus	67.57	-139.83	Beta-13867	13820	840	18890	14225	16729	√
Mammuthus	67.13	-140.78	RIDDL-559	13940	160	17406	16397	16903	√
Mammuthus	69.99	-151.62	Beta-283246	14070	60	17380	16864	17106	√
Mammuthus	65.10	-147.30	AA-14892	14093	163	17591	16606	17132	√
Mammuthus	65.80	-163.20	Beta-20027	14270	950	19984	14750	17331	√
Mammuthus	64.74	-155.49	AA-26002	14300	170	17889	16949	17409	√
Mammuthus	64.40	-141.23	AA-14919	14372	92	17811	17214	17516	√
Mammuthus	65.12	-147.53	AA-14923	14390	92	17839	17245	17539	√
Mammuthus	60.50	-149.86	AA-14882	14679	174	18312	17460	17866	√
Mammuthus	64.74	-155.49	AA-26030	14760	170	18380	17554	17967	√
Mammuthus	63.57	-156.01	Beta-5691	15090	170	18706	17946	18333	√
Mammuthus	65.12	-147.53	AA-14912	15102	135	18659	18003	18349	√
Mammuthus	60.50	-149.86	AA-14932	15373	101	18845	18408	18643	√
Mammuthus	64.94	-147.79	AA-14941	15426	98	18890	18485	18693	√
Mammuthus	60.50	-149.86	AA-14920	15453	99	18913	18512	18717	√
Mammuthus	65.12	-147.53	AA-14910	15513	192	19222	18353	18777	√
Mammuthus	60.50	-149.86	AA-14894	15540	145	19136	18501	18799	√
Mammuthus	68.14	-165.98	AA-22619	15654	218	19489	18493	18936	√
Mammuthus	68.35	-166.76	AA-26015	15740	230	19584	18560	19037	√
Mammuthus	65.05	-147.35	CAMS-9898	15830	70	19302	18895	19084	√
Mammuthus	64.94	-147.79	AA-14872	15796	195	19560	18690	19088	√
Mammuthus	65.12	-147.53	AA-14866	16168	209	20027	18990	19511	√
Mammuthus	65.20	-165.48	AA-14364	16319	292	20415	18990	19704	√
Mammuthus	65.43	-165.78	AA-17571	16940	210	20988	19927	20437	√
Mammuthus	70.05	-162.46	Shell-6713A	17300	800	22960	19095	20995	
Mammuthus	64.94	-147.79	AA-14922	17437	132	21464	20676	21061	√
Mammuthus	67.13	-140.78	CRNL-1221	17880	330	22423	20826	21639	√
Mammuthus	67.13	-140.78	RIDDL-330	17880	330	22423	20826	21639	√

Mammuthus	69.50	-154.40	CAMS-120653[#]	17870	60	21865	21435	21661	√
Mammuthus	69.50	-154.40	CAMS-121739[#]	17965	50	21945	21563	21767	√
Mammuthus	64.05	-139.42	Beta-70099	18030	120	22221	21507	21845	√
Mammuthus	58.30	-135.00	AA-26004	18090	250	22470	21270	21916	√
Mammuthus	65.11	-153.34	AA-26021	18140	280	22567	21227	21969	√
Mammuthus	67.08	-158.17	USGS-1485	18560	70	22599	22285	22433	
Mammuthus	67.08	-158.17	USGS-1439	19060	90	23300	22638	22950	
Mammuthus	69.50	-154.40	CAMS-92087	19530	80	23818	23210	23533	√
Mammuthus	69.50	-154.40	AA-17620	19560	330	24352	22774	23561	√
Mammuthus	67.13	-140.78	RIDDL-330 - MgVo-1	19640	170	24078	23174	23661	√
Mammuthus	64.93	-161.15	AA-14356	19763	307	24521	23012	23796	√
Mammuthus	69.50	-154.40	AA-17623	19970	350	25040	23191	24053	√
Mammuthus	70.22	-151.06	Beta-192036	20150	110	24500	23934	24218	√
Mammuthus	65.25	-166.86	AA-26003	20120	350	25216	23431	24241	√
Mammuthus	67.13	-140.78	RIDDL-223	20230	180	24918	23888	24323	√
Ovibos	70.90	-155.96	OxA-23706	224	23	308	…	182	√
Ovibos	70.35	-156.77	AA-48776	226	59	456	…	212	√
Ovibos	70.17	-147.30	Beta-339445	250	30	429	…	295	√
Ovibos	70.17	-147.30	Beta-339278	340	30	481	311	390	√
Ovibos	70.27	-151.01	Beta-283248	350	40	495	312	399	√
Ovibos	70.17	-154.11	Beta-244761	900	40	916	735	826	√
Ovibos	69.60	-139.10	Beta-179008	1020	40	1051	799	939	√
Ovibos	70.17	-154.11	Beta-244762	1080	40	1066	926	990	√
Ovibos	69.60	-139.10	AAR12041	1100	40	1173	929	1008	√
Ovibos	70.17	-154.11	Beta-223266	1140	40	1175	965	1049	√
Ovibos	70.35	-156.77	AA-48283	1148	42	1177	969	1062	√
Ovibos	63.18	-139.00	I-3568	2910	100	3342	2799	3060	
Ovibos	64.02	-140.87	I-10985	3360	90	3834	3400	3606	
Ovibos	63.72	-138.62	OxA-22318	6739	37	7668	7521	7602	√
Ovibos	69.50	-154.40	AA-48263	7127	59	8148	7799	7953	√
Ovibos	64.05	-139.44	AAR11743	9280	60	10649	10264	10460	√
Ovibos	69.50	-154.40	AA-48757	10180	110	12379	11356	11845	√
Ovibos	69.60	-139.10	AAR12052	12600	100	15263	14354	14909	√
Ovibos	69.60	-139.10	AAR11756	12590	75	15217	14464	14919	√
Ovibos	64.93	-147.64	OxA-22821	12740	50	15350	14986	15181	√

Ovibos	69.57	-138.92	Beta-71232	13300	60	16205	15779	15995	√
Ovibos	67.13	-140.78	RIDDL-557	14370	130	17872	17139	17509	√
Ovibos	69.60	-139.10	AAR11718	14770	120	18292	17666	17976	√
Ovibos	69.60	-139.10	OxA-17070	17265	65	21043	20607	20818	√
Ovibos	69.60	-139.10	AAR11735	20080	150	24516	23775	24149	√
Ovibos	69.54	-156.06	Beta-223267	21050	90	25640	25155	25405	√
Rangifer	65.04	-147.11	AA-85596	112	44	275	9	122	√
Rangifer	64.08	-139.43	AA-83810	115	44	275	9	124	√
Rangifer	65.58	-139.08	Beta-70225	140	50	284	...	143	√
Rangifer	69.50	-154.40	CAMS-64413	160	40	288	...	168	√
Rangifer	60.78	-150.52	RIDDL-552	160	90	429	...	171	√
Rangifer	60.58	-131.30	Beta-212882	190	40	306	...	177	√
Rangifer	61.04	-136.87	Beta-212897	190	40	306	...	177	√
Rangifer	69.50	-154.40	CAMS-64409	200	50	420	...	181	√
Rangifer	69.50	-154.40	CAMS-64416	220	40	426	...	191	√
Rangifer	69.33	-138.00	RIDDL-542	200	90	452	...	198	√
Rangifer	64.08	-139.43	AA-84483	220	120	471	...	236	√
Rangifer	69.33	-138.00	RIDDL-365	260	120	503	...	293	√
Rangifer	64.08	-139.43	AA-84498	255	43	460	...	303	√
Rangifer	60.78	-150.52	RIDDL-553	290	90	514	...	348	√
Rangifer	69.50	-154.40	CAMS-64465	350	30	492	315	395	√
Rangifer	65.58	-139.08	Beta-70226	350	50	499	308	400	√
Rangifer	60.40	-135.45	Beta-162895	360	40	500	315	408	√
Rangifer	65.58	-139.08	Beta-64368	410	75	547	302	443	√
Rangifer	69.50	-154.40	CAMS-64403	390	40	514	316	448	√
Rangifer	69.35	-132.67	RIDDL-344	490	170	786	...	496	√
Rangifer	69.17	-132.50	RIDDL-547	500	90	664	318	529	√
Rangifer	68.92	-136.42	RIDDL-363	600	130	792	317	596	√
Rangifer	69.40	-140.50	I-18243	650	80	726	522	615	
Rangifer	68.83	-135.25	RIDDL-548	740	120	915	536	698	√
Rangifer	61.29	-138.00	Beta-217505	790	40	781	670	712	√
Rangifer	67.13	-163.75	S-3369	850	75	919	675	778	
Rangifer	69.57	-138.92	Beta-79850 CAMS-18413	1070	50	1173	835	985	√
Rangifer	69.50	-154.40	CAMS-64397	1120	40	1174	938	1026	√

Rangifer	69.50	-154.40	CAMS-64462	1190	30	1229	1005	1119	√
Rangifer	67.85	-139.77	RIDDL-145	1350	150	1555	958	1261	√
Rangifer	69.43	-160.91	GaK-2304	1470	80	1544	1270	1378	
Rangifer	68.36	-166.75	P-98	1619	210	2036	1081	1552	√
Rangifer	67.58	-139.75	RIDDL-140	1730	100	1870	1413	1650	√
Rangifer	67.13	-163.75	S-3368	1810	160	2122	1386	1743	
Rangifer	67.48	-139.72	RIDDL-141	1880	140	2295	1424	1820	√
Rangifer	60.39	-135.44	Beta-162887	1940	40	1994	1815	1890	√
Rangifer	69.97	-148.87	Uga-3719	2075	70	2304	1881	2050	√
Rangifer	69.50	-154.40	CAMS-64453	2140	40	2305	2000	2128	√
Rangifer	60.39	-135.44	Beta-162889	2320	40	2460	2163	2339	√
Rangifer	60.40	-135.45	Beta-162886	2340	40	2672	2185	2356	√
Rangifer	60.39	-135.44	Beta-162888	2510	40	2745	2458	2589	√
Rangifer	60.39	-135.44	Beta-162893	2550	40	2755	2491	2630	√
Rangifer	65.80	-163.22	K-147	2620	120	2969	2356	2715	
Rangifer	69.50	-154.40	CAMS-64420	2600	40	2788	2505	2741	√
Rangifer	60.17	-136.91	Beta-212884	2700	40	2870	2750	2804	√
Rangifer	65.80	-163.22	K-983	2700	110	3142	2490	2827	
Rangifer	68.18	-139.96	RIDDL-133	2930	140	3396	2771	3091	√
Rangifer	68.20	-151.62	SM-917	3042	188	3641	2779	3223	
Rangifer	60.60	-136.26	Beta-162894	3140	40	3450	3246	3363	√
Rangifer	60.39	-135.44	Beta-162885	3150	40	3454	3250	3375	√
Rangifer	60.39	-135.44	Beta-162897	3220	40	3559	3367	3439	√
Rangifer	69.00	-132.00	RIDDL-546	3160	800	5608	1621	3520	√
Rangifer	69.36	-139.53	P-228	3288	156	3962	3084	3532	√
Rangifer	61.27	-138.08	Beta-212894	3480	40	3849	3640	3756	√
Rangifer	60.40	-135.45	Beta-152439	3720	40	4224	3929	4061	√
Rangifer	60.39	-135.44	Beta-162892	3740	40	4234	3978	4095	√
Rangifer	60.39	-135.44	Beta-162882	3760	40	4242	3985	4123	√
Rangifer	61.27	-138.08	Beta-227525	3790	40	4350	3995	4174	√
Rangifer	61.27	-138.08	Beta-227526	3820	40	4406	4091	4217	√

Rangifer	56.94	-130.35	S-2279	3840	70	4426	3998	4253	
Rangifer	60.39	-135.44	Beta-162884	3890	40	4423	4160	4326	√
Rangifer	61.29	-138.00	Beta-212895	4190	40	4844	4584	4724	√
Rangifer	60.60	-136.26	Beta-162890	4760	40	5590	5329	5513	√
Rangifer	61.27	-138.08	Beta-212896	4830	40	5647	5472	5545	√
Rangifer	60.31	-136.00	Beta-152440	5000	40	5892	5644	5730	√
Rangifer	63.80	-139.07	I-8642	5090	100	6173	5602	5826	
Rangifer	60.34	-136.06	Beta-162883	5710	40	6631	6408	6497	√
Rangifer	60.31	-136.00	Beta-162891	6320	40	7409	7163	7250	√
Rangifer	67.86	-139.80	I-4221	6530	135	7660	7175	7433	
Rangifer	69.50	-154.40	CAMS-64395	7830	40	8761	8523	8608	√
Rangifer	69.50	-154.40	CAMS-64463	8830	40	10152	9704	9895	√
Rangifer	69.50	-154.40	CAMS-64454	8890	50	10191	9785	10022	√
Rangifer	56.17	-133.50	AA-18449	10515	90	12675	12119	12452	√
Rangifer	56.17	-133.50	AA-18449R	10555	110	12707	12130	12486	√
Rangifer	64.08	-139.43	AA-84496	11020	110	13076	12719	12895	√
Rangifer	69.93	-138.98	Beta-27512 ETH-4582	11350	110	13434	13034	13205	√
Rangifer	67.13	-140.78	RIDDL-277	12210	210	15054	13624	14230	√
Rangifer	69.50	-154.40	CAMS-64410	12370	50	14740	14129	14402	√
Rangifer	69.50	-154.40	Beta-117140	12710	100	15513	14689	15123	√
Rangifer	67.13	-140.78	CAMS-23468	12830	60	15565	15115	15294	√
Rangifer	61.75	-155.50	Beta-67671	13130	180	16246	15224	15742	√
Rangifer	69.50	-154.40	CAMS-64470	13250	50	16114	15739	15928	√
Rangifer	64.08	-139.43	AA-84497	13930	150	17375	16405	16888	√
Rangifer	69.50	-154.40	CAMS-64408	14380	50	17711	17320	17527	√
Rangifer	64.93	-147.64	AA-83815	14610	160	18202	17396	17785	√
Rangifer	61.75	-155.50	Beta-67669	15690	140	19315	18655	18952	√
Rangifer	69.50	-154.40	CAMS-64417	16950	50	20620	20245	20446	√
Rangifer	64.81	-164.50	AA-83813	17430	220	21692	20510	21067	√
Rangifer	64.07	-141.89	AA-84481	17440	190	21618	20571	21076	√
Rangifer	69.50	-154.40	CAMS-64415	17610	60	21534	21024	21290	√

Rangifer	69.50	-154.40	CAMS-64456	18410	60	22464	22041	22307	√
Rangifer	64.07	-141.89	AA-83818	18570	250	23016	21861	22442	√
Rangifer	65.61	-164.80	AA-84480	19370	220	23910	22800	23331	√
Rangifer	66.00	-141.00	AA-83812	19720	330	24537	22924	23748	√
Rangifer	69.50	-154.40	CAMS-64398	20480	80	24996	24341	24639	√
Saiga	64.07	-141.89	AA-3075	12390	120	15042	14075	14502	√
Saiga	63.98	-141.99	OxA-23696	12460	55	14995	14242	14612	√
Saiga	64.07	-141.89	AA-3074	12620	110	15305	14337	14938	√
Saiga	63.98	-141.99	OxA-23697	12645	55	15235	14755	15040	√
Saiga	65.04	-147.11	AA-3215	12780	140	15751	14682	15232	√
Saiga	67.57	-139.83	Beta-79853, CAMS-18416)	13220	70	16125	15660	15891	√
Saiga	67.13	-140.80	RIDDL-279	13390	180	16691	15579	16115	√

Supplementary Table 3: Core sediment description

Core	Sediments
Windmill Lake	The core is 460cm long and the samples utilised for this work span 320-445cm below sediment surface. The core base consists of pebbles, silt and sand, followed above ca. 440cm, by silty sediments. From 405cm upwards the sediments become increasingly organic and from 290 cm upwards the sediments consist of gyttja. At 173cm the Jarvis Creek Ash can be identified as a 1mm-thick layer.
Jan Lake	The core is 364cm long and the samples utilised for this work span 151-348cm below sediment surface. Sediment in the lowest part of the core (363 to 249cm) is dense, dry silt. Above a core break between 249-233cm, the sediments are dark brownish black silty gyttja with laminations present throughout this part of the record. Two tephras at 138 and 149cm are thought to correlate with the Jarvis Ash. Organic matter (loss-on-ignition, LOI) is <10% until it rises above 10% from 300cm and >25% above 233 cm depth.
Ruppert Lake	The core is 396cm long and the samples utilised for this work span 0-387cm below sediment surface. The sediments in the lowest part of the core (353 to 396cm) consist of intermittent silty, sandy and coarse sandy layers. From 353 cm upwards the sediments become increasingly organic (LOI increase from 15% to 35%). This highly organic sediment contains ~60 bands of silty clay varying in thickness between 1 and 10mm thick throughout the upper 300cm of the core and a layer of moss remains at 165 cm depth.
Woody Bottom Pond	The core is 205cm long and the samples utilised for this work span 0-200cm below sediment surface. It consists mainly of gyttja (LOI between 50-80%). The lowest part of the core (175 to 205 cm) and the top part of the core (0 to 50 cm) contain a greater minerogenic component (LOI values are relatively low, <60%, and Ti and Fe values from XRF analysis are high, compared with the middle part of the record (M. van Hardenbroek, unpublished data)). There is a distinct layer of moss remains at 188 cm depth.

Supplementary Figure 1: Core stratigraphy and age-depth models

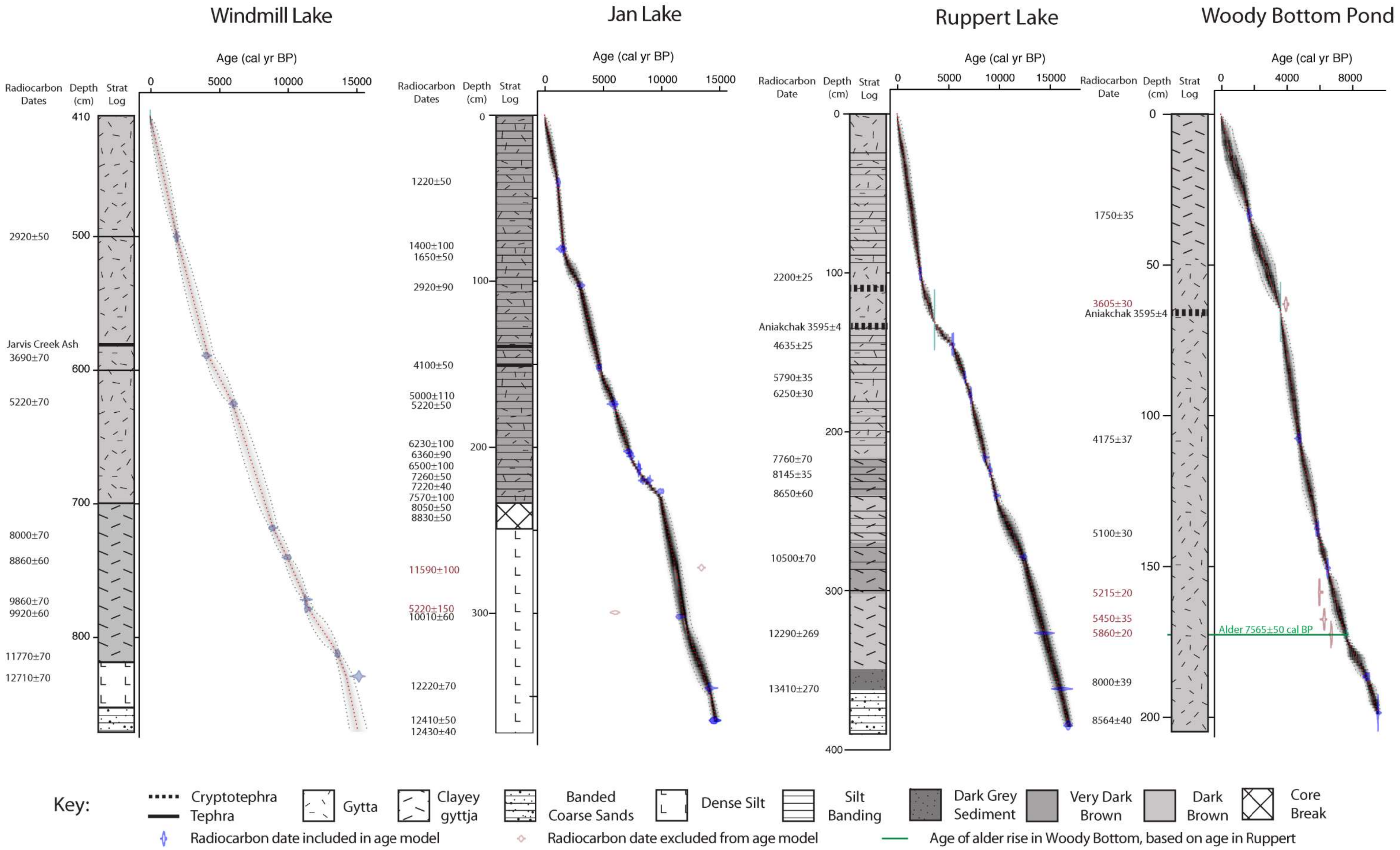

Supplementary Figures 2-5: Spore accumulation rates compared to spore percentage, relative to pollen sum

For figure 2-5 the legend as follows applies: blue = spore accumulation rates (AR), red = percent relative to pollen sum (%). Total dung fungal spores accumulation rates include: *Sporormiella*, *Sordaria* and *Podospora* spore types

Supplementary Figure 2: Jan Lake

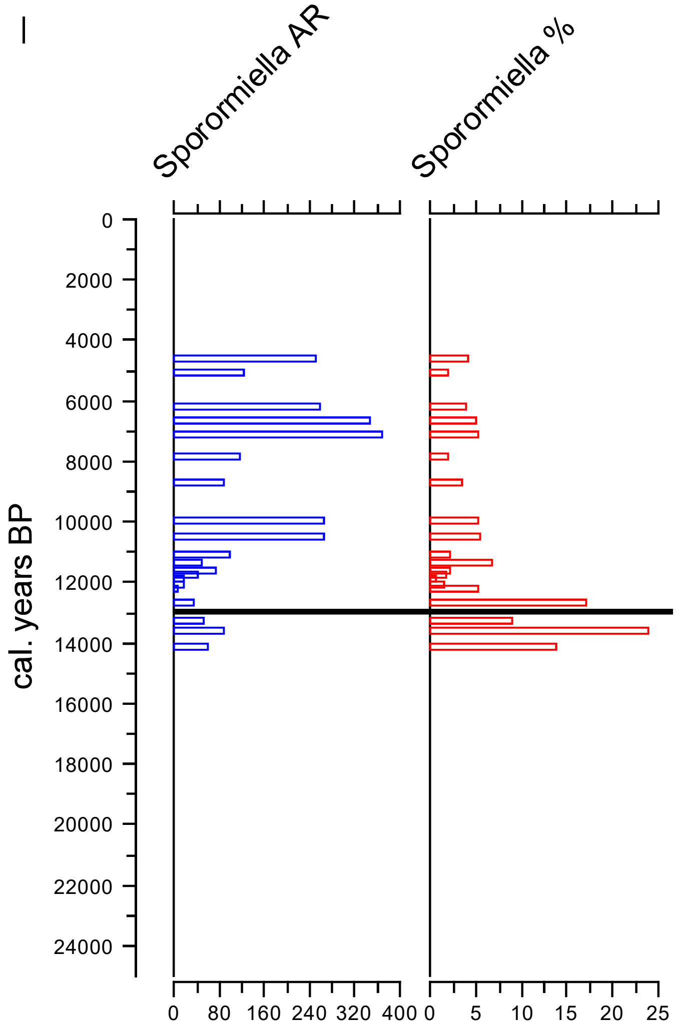

Supplementary Figure 3: Windmill Lake

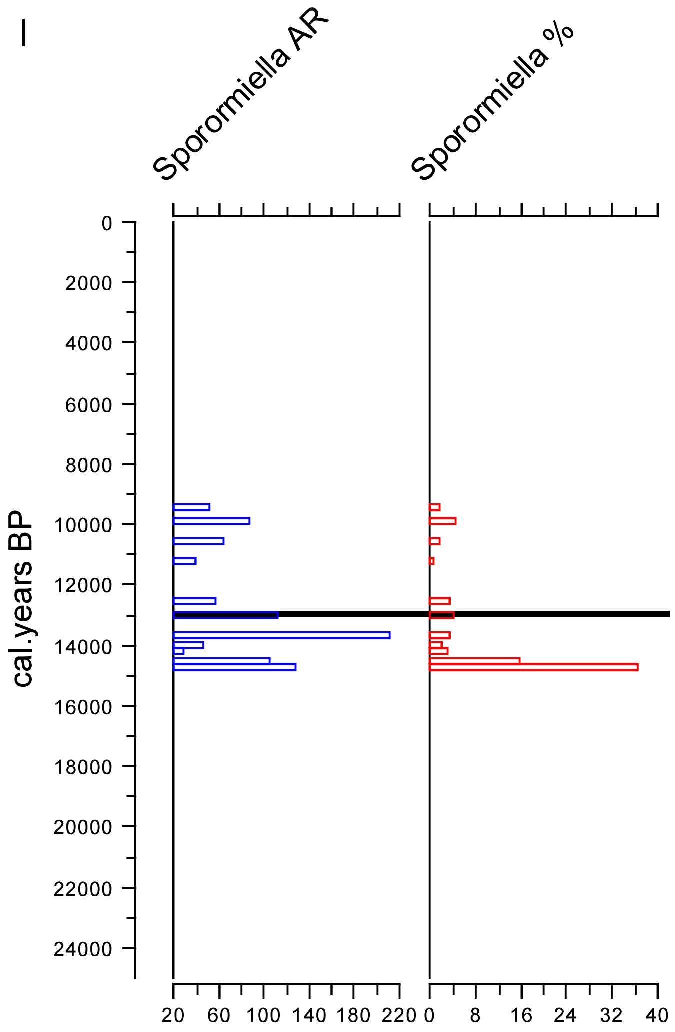

Supplementary Figure 4: Ruppert Lake

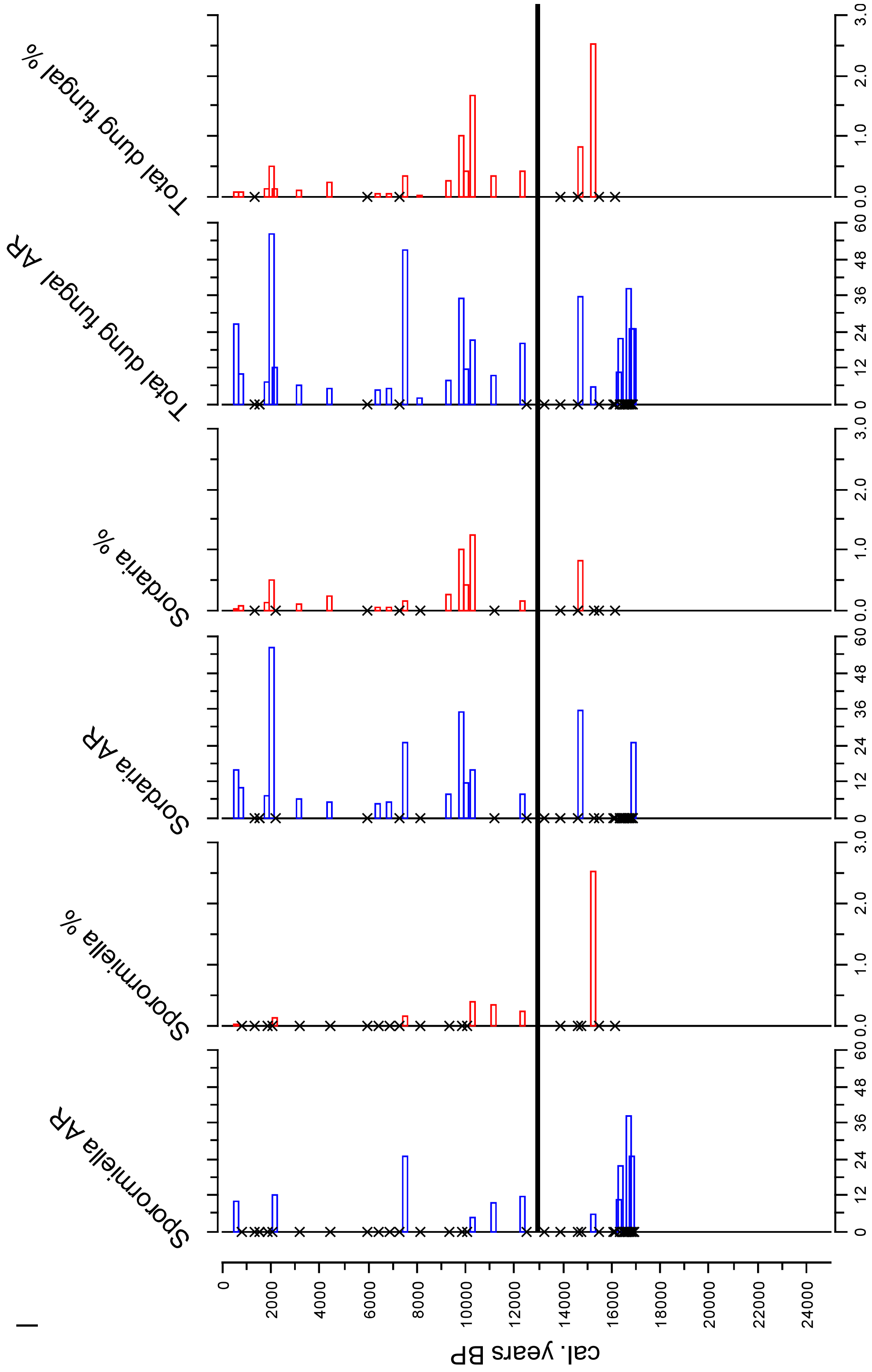

Supplementary Figure 5: Woody Bottom Pond